

Generalized probabilistic principal component analysis of correlated data

Mengyang Gu* and Weining Shen**

*Department of Applied Mathematics and Statistics,
Johns Hopkins University

**Department of Statistics, University of California, Irvine

Abstract

Principal component analysis (PCA) is a well-established tool in machine learning and data processing. Tipping and Bishop (1999) proposed a probabilistic formulation of PCA (PPCA) by showing that the principal axes in PCA are equivalent to the maximum marginal likelihood estimator of the factor loading matrix in a latent factor model for the observed data, assuming that the latent factors are independently distributed as standard normal distributions. However, the independence assumption may be unrealistic for many scenarios such as modeling multiple time series, spatial processes, and functional data, where the output variables are correlated.

In this paper, we introduce the generalized probabilistic principal component analysis (GPPCA) to study the latent factor model of multiple correlated outcomes, where each factor is modeled by a Gaussian process. The proposed method provides a probabilistic solution of the latent factor model with the scalable computation. In particular, we derive the maximum marginal likelihood estimator of the factor loading matrix and the predictive distribution of the output. Based on the explicit expression of the precision matrix in the marginal likelihood, the number of the computational operations is linear to the number of output variables. Moreover, with the use of the Matérn covariance function, the number of the computational operations is also linear to the number of time points for modeling the multiple time series without any approximation to the likelihood function. We discuss the connection of the GPPCA with other approaches such as the PCA and PPCA, and highlight the advantage of GPPCA in terms of the practical relevance, estimation accuracy and computational convenience. Numerical studies confirm the excellent finite-sample performance of the proposed approach.

KEYWORDS: Gaussian process, maximum marginal likelihood estimator, principal component analysis, Stiefel manifold

1 Introduction

Principal component analysis (PCA) is one of the oldest and most widely known approaches for dimension reduction. It has been widely used in many applications, including exploratory data analysis, regression, time series analysis, image processing, and functional data analysis. The most common solution of the PCA is to find a linear projection that transforms the set of original correlated variables onto a projected space of new uncorrelated variables by maximizing the variation of the projected space (Jolliffe, 2011). This solution, despite its wide use in practice, lacks a probabilistic description of the data.

A probabilistic formulation of the PCA was first introduced by Tipping and Bishop (1999), where the authors considered a Gaussian latent factor model, and then obtained the PCA (principal axes) as the solution of a maximum marginal likelihood problem, where the latent factors were marginalized out. This approach, known as the probabilistic principal component analysis (PPCA), assumes that the latent factors are independently distributed following a standard normal distribution. However, the independence assumption of the factors is usually too restrictive for many applications, where the variables of interest are correlated between different inputs, e.g. times series, image studies, and spatial statistics. A few efforts have been made to extend the latent factor model to incorporate the dependent structure of the factors in the literature. For example, the linear model of coregionalization (LMC) is studied in modeling multivariate outputs of spatially correlated data (Gelfand et al., 2004, 2010), where each factor is modeled as a Gaussian process (GP) to account for the spatial correlation in the data. When the loading matrix is shared, the LMC becomes the semiparametric latent factor model, introduced in machine learning (Seeger et al., 2005; Álvarez et al., 2011) and is widely applied in emulating computationally expensive computer models with multivariate outputs (Higdon et al., 2008; Fricker et al., 2013; Gu and Berger, 2016), where each factor is modeled by a GP over a p -dimensional input.

In this work, we propose a new approach called generalized probabilistic principal component analysis (GPPCA), as an extension of the PPCA for the correlated output data. We assume each column of the factor loading matrix is orthonormal for the identifiability purpose. Based on this assumption, we obtain a closed-form solution for the maximum marginal likelihood estimation of the factor loading matrix when the covariance function of the factor processes is shared. This result is an extension of the PPCA for the correlated factors, and the connection between these two approaches is studied. When the covariance functions of the factor processes are different, the maximum marginal likelihood estimation of the factor loading matrix is equivalent to an optimization problem with orthogonal constraints, sometimes referred as the Stiefel manifold, and a fast numerical search algorithm for this optimization problem is used (Wen and Yin, 2013).

We also derive the maximum marginal likelihood estimator of the variance of the noise and the parameters in the covariance functions. We feature the computational advantages of our approach. Note that the latent factor model with each factor modeled as a GP is known as a nonseparable model, since the covariance matrix cannot be decomposed as a Kronecker product of two small matrices (Álvarez et al., 2011). We show that the computational operations of each evaluation of the likelihood of the nonseparable model in our study are linear to the number of variables in the output data, which is the same as the one in the separable model, because the inverse of the covariance matrix is shown to have an explicit

expression. When the input is a scalar, the computational operations of the likelihood and the predictive distribution of the output are linear to the number of the inputs when the Matérn covariance function is used. All these computational advantages do not rely on approximating the covariance matrix or the likelihood of the GP, which makes it distinct to some commonly used approaches in the GP literature.

There are several approaches of estimating the factor loading matrix in the latent factor model and semiparametric latent factor model in the Frequentist and Bayesian literature. One of the most popular approaches for estimating the factor loading matrix is PCA (see e.g. Bai and Ng (2002); Bai (2003); Higdon et al. (2008)). Under the orthonormal assumption of each factor loading vector, the PCA can be obtained from the maximum likelihood estimator of the factor loading matrix. However, the correlation structure of each factor is not incorporated for the estimation. Our GPPCA can be viewed as a better alternative by putting a sensible prior for the factor processes and the prior is marginalized out to obtain the estimator of the factor loadings. In Lam et al. (2011) and Lam and Yao (2012), another estimator of the factor loading matrix is derived based on the sample covariance of the output data at the first several time lags when modeling high-dimensional time series. We will numerically compare our approach to the aforementioned Frequentist approaches.

The Bayesian priors of the factor loading matrix are also widely studied in recent works. In West (2003), the PCA is connected to a class of the generalized singular g-prior in the regression and a spike and slab prior that induces the sparse factors in the latent factor model is introduced, assuming the factors are independently distributed. Another prior of the factor loading matrix that induces the sparsity is introduced by Bhattacharya and Dunson (2011) with the independent factors and its asymptotic behaviors are also discussed. Nakajima and West (2013); Zhou et al. (2014) introduce a direct method to threshold the time-varying factor loading matrix in Bayesian dynamic linear models. In modeling spatially correlated data, priors are also discussed for the spatially varying factor loading matrices (Gelfand et al., 2004) in LMC. Our results of the closed-form marginal likelihood of the latent factor model with dependent factors may be extended to derive new prior distributions for the factor loading matrix.

The rest of the paper is organized as follows. The main results of the closed-form marginal likelihood and the maximum marginal likelihood estimator of the factor loading matrix are introduced in Section 2.1. In Section 2.2, we provide the maximum marginal likelihood estimator for the noise parameter and kernel parameters, after marginalizing out the factor processes. The comparison between our approach and other approaches in estimating the factor loading matrix is studied in Section 3, with a focus on the connection of the GPPCA and PPCA. The numerical results are provided in Section 4, for both the correctly specified and misspecified models with unknown noise and covariance parameters. We conclude this work with several potential extensions in Section 5.

2 Main results

2.1 Generalized probabilistic principal component analysis

To begin with, let $\mathbf{y}(\mathbf{x}) = (y_1(\mathbf{x}), \dots, y_k(\mathbf{x}))^T$ be a k -dimensional real-valued output vector at a p -dimensional input vector \mathbf{x} . Let $\mathbf{Y} = [\mathbf{y}(\mathbf{x}_1), \dots, \mathbf{y}(\mathbf{x}_n)]$ be a $k \times n$ matrix of the observations at inputs $\{\mathbf{x}_1, \dots, \mathbf{x}_n\}$. Without the loss of the generality, we assume the each row of the \mathbf{Y} is centered at zero. If not, we may normalize each row of the output by its mean of the row.

Consider the following latent factor model

$$\mathbf{y}(\mathbf{x}) = \mathbf{A}\mathbf{z}(\mathbf{x}) + \boldsymbol{\epsilon}, \quad (1)$$

where $\boldsymbol{\epsilon} \sim N(0, \sigma_0^2 \mathbf{I}_k)$ is a vector of the independent normally distributed noises, with \mathbf{I}_k being the $k \times k$ identity matrix. The $k \times d$ factor loading matrix $\mathbf{A} = [\mathbf{a}_1, \dots, \mathbf{a}_d]$ relates the k -dimensional outputs to a d -dimensional factor processes $\mathbf{z}(\mathbf{x}) = (z_1(\mathbf{x}), \dots, z_d(\mathbf{x}))^T$, where $d \leq k$.

In many applications, each output is correlated. For example, model (1) is widely used in analyzing multiple time series, where $y_l(x)$'s are correlated across different values of time points for $l = 1, \dots, k$. Model (1) is also used for analyzing multivariate outputs from spatially correlated data, often referred as the linear model of coregionalization (LMC) (Gelfand et al., 2010). In these studies, a popular approach is to model each factor by a zero-mean Gaussian process (GP), meaning that for any set of inputs $\{\mathbf{x}_1, \dots, \mathbf{x}_n\}$, $\mathbf{Z}_l = (z_l(\mathbf{x}_1), \dots, z_l(\mathbf{x}_n))$ follows a multivariate normal distribution

$$\mathbf{Z}_l^T \sim \text{MN}(\mathbf{0}, \boldsymbol{\Sigma}_l), \quad (2)$$

where the (i, j) entry of $\boldsymbol{\Sigma}_l$ is parameterized by a kernel function $K_l(\mathbf{x}_i, \mathbf{x}_j)$ for $l = 1, \dots, d$ and $1 \leq i, j \leq n$. We defer the discussion of the kernel in the Section 2.2.

Denote the vectorization of the output $\mathbf{Y}_v = \text{vec}(\mathbf{Y})$ and the $d \times n$ latent factor matrix $\mathbf{Z} = (\mathbf{z}(\mathbf{x}_1), \dots, \mathbf{z}(\mathbf{x}_n))$ at inputs $\{\mathbf{x}_1, \dots, \mathbf{x}_n\}$. After marginalizing out \mathbf{Z} , the distribution of \mathbf{Y} follows a multivariate normal distribution as follows

$$\mathbf{Y}_v \mid \mathbf{A}, \sigma_0^2, \boldsymbol{\Sigma}_1, \dots, \boldsymbol{\Sigma}_d \sim \text{MN} \left(\mathbf{0}, \sum_{l=1}^d \boldsymbol{\Sigma}_l \otimes (\mathbf{a}_l \mathbf{a}_l^T) + \sigma_0^2 \mathbf{I}_{nk} \right), \quad (3)$$

for $l = 1, \dots, d$. The form in (3) appears in the previous literature (e.g. Gelfand et al. (2004)) and we also derive it in Appendix B.

Note that the model (1) is unchanged if one replaces the pair $(\mathbf{A}, \mathbf{z}(\mathbf{x}))$ by $(\mathbf{A}\mathbf{H}, \mathbf{H}^{-1}\mathbf{z}(\mathbf{x}))$ for any invertible matrix \mathbf{H} . Due to this reason, one often assumes the columns of \mathbf{A} are orthonormal (Lam et al., 2011; Lam and Yao, 2012).

Assumption 1.

$$\mathbf{A}^T \mathbf{A} = \mathbf{I}_d. \quad (4)$$

Under the Assumption 1, the d -dimensional linear space specified by the column space \mathbf{A} , denoted as $\mathcal{M}(\mathbf{A})$, is uniquely determined by the model (1). With this assumption, we are able to express the marginal distribution for \mathbf{Y}_v explicitly in the following Lemma 1.

Lemma 1. *Under Assumption 1, the marginal distribution of \mathbf{Y}_v in model (1) is the multivariate normal distribution as follows*

$$\mathbf{Y}_v \mid \mathbf{A}, \sigma_0^2, \Sigma_1, \dots, \Sigma_d \sim \text{MN} \left(\mathbf{0}, \sigma_0^2 \left(\mathbf{I}_{nk} - \sum_{l=1}^d (\sigma_0^2 \Sigma_l^{-1} + \mathbf{I}_n)^{-1} \otimes (\mathbf{a}_l \mathbf{a}_l^T) \right)^{-1} \right), \quad (5)$$

for $l = 1, \dots, d$.

Equation (5) is seemingly more complicated than the expression in (3) for the marginal distribution for \mathbf{Y}_v . It is useful because it gives an explicit form of the precision matrix (i.e. the inverse of the covariance matrix) of \mathbf{Y}_v , which allows us to derive the maximum marginal likelihood estimator for \mathbf{A} and other parameters without inverting an $nk \times nk$ covariance matrix. The following theorem gives the maximum marginal estimation of \mathbf{A} where the covariance matrix for each latent factor is shared.

Theorem 1. *For model (1), assume $\Sigma_1 = \dots = \Sigma_d = \Sigma$. Under Assumption 1, after marginalizing out \mathbf{Z} , the likelihood function is maximized when*

$$\hat{\mathbf{A}} = \mathbf{U} \mathbf{R} \quad (6)$$

where \mathbf{U} is a $k \times d$ matrix of the first d principal eigenvectors of

$$\mathbf{G} = \mathbf{Y}(\sigma_0^2 \Sigma^{-1} + \mathbf{I}_n)^{-1} \mathbf{Y}^T, \quad (7)$$

and \mathbf{R} is an arbitrary $d \times d$ orthogonal rotation matrix.

By theorem 1, the solution for \mathbf{A} is not unique because of the arbitrary rotation matrix. However, the linear subspace of the column space of the estimated factor loading matrix, denoted as $\mathcal{M}(\hat{\mathbf{A}})$, is uniquely determined by (6).

In general, the covariance function of each factor can be different. We are able to express the maximum marginal likelihood estimator as the solution to a closed-form optimization problem with the orthogonal constraints, stated in the following Theorem 2.

Theorem 2. *Under Assumption 1, after marginalizing out \mathbf{Z} , the maximum marginal likelihood estimator of \mathbf{A} in model (1) is*

$$\hat{\mathbf{A}} = \underset{\mathbf{A}}{\operatorname{argmax}} \sum_{l=1}^d \mathbf{a}_l^T \mathbf{G}_l \mathbf{a}_l, \quad \text{s.t.} \quad \mathbf{A}^T \mathbf{A} = \mathbf{I}_d, \quad (8)$$

where

$$\mathbf{G}_l = \mathbf{Y}(\sigma_0^2 \Sigma_l^{-1} + \mathbf{I}_n)^{-1} \mathbf{Y}^T. \quad (9)$$

The subset of matrices \mathbf{A} that satisfies the orthogonal constraint $\mathbf{A}^T \mathbf{A} = \mathbf{I}_d$ is often referred as the *Stiefel manifold*. Unlike the case where the covariance of each factor processes is shared, no closed-form solution of the optimization problem in (2) was found. A numerical optimization algorithm that preserves the orthogonal constraints in (8) is introduced in Wen and Yin (2013). The main idea of the algorithm is to find the gradient of the objective function in the tangent space at the current step, and iterates by a curve along the projected negative descent on the manifold. The curvilinear search is applied to find the appropriate step size that guarantees the convergence to a stationary point. We implement this approach to numerically optimize the marginal likelihood to obtain the estimation of the factor loading matrix in Theorem 2.

We call the method of estimating \mathbf{A} in Theorem 1 and Theorem 2 the generalized probabilistic principal component analysis (GPPCA) of correlated data, which is a direct extension of the PPCA in Tipping and Bishop (1999). Although both approaches obtain the maximum marginal likelihood estimator of the factor loading matrix, after integrating out the latent factors, the key difference is that in GPPCA, the latent factors at different inputs are allowed to be correlated, whereas the latent factors in PPCA are assumed to be independent. A detailed numerical comparison between our method and other approaches including the PPCA will be given in Section 3.

Another nice feature of the proposed GPPCA method is that the estimation of the factor loading matrix can be applied to any covariance structure of the factor processes. In this paper, we use kernels to parameterize the covariance matrix as an illustrative example. There are many other ways to specify the covariance matrix or the inverse of the covariance matrix, such as the Markov random field and the dynamic linear model, and these approaches are readily applicable in our latent factor model (1).

2.2 Parameter estimation and predictive distribution

Once we obtain the probabilistic estimation of the factor loading matrix \mathbf{A} in model (1) based on Theorems 1 and 2, it is natural to consider the estimation of remaining parameters, which, in our case, includes a noise parameter σ_0^2 and the parameters in the kernel functions.

In analyzing spatially correlated data, one often utilizes an isotropic covariance function, meaning that the kernel is a function of the Euclidean distance between the spatial coordinates. For a function with a p -dimensional input, a product kernel is often assumed (Sacks et al., 1989), meaning that for the l th factor

$$K_l(\mathbf{x}_a, \mathbf{x}_b) = \sigma_l^2 \prod_{m=1}^p K_{lm}(x_{am}, x_{bm}), \quad (10)$$

for any input $\mathbf{x}_a = (x_{a1}, \dots, x_{ap})$ and $\mathbf{x}_b = (x_{b1}, \dots, x_{bp})$, where $K_{lm}(\cdot, \cdot)$ is a one-dimensional kernel function that models the correlation of the m th coordinate of the l th factor vector at any two inputs.

Some widely used one-dimensional kernel functions include the power exponential kernel and the Matérn kernel. For any two inputs $\mathbf{x}_a, \mathbf{x}_b \in \mathcal{X}$, the Matérn kernel is

$$K_{lm}(x_{am}, x_{bm}) = \frac{1}{2^{\nu_{lm}-1} \Gamma(\nu_{lm})} \left(\frac{|x_{am} - x_{bm}|}{\gamma_{lm}} \right)^{\nu_{lm}} \mathcal{K}_{\nu_{lm}} \left(\frac{|x_{am} - x_{bm}|}{\gamma_{lm}} \right), \quad (11)$$

where $\Gamma(\cdot)$ is the gamma function and $\mathcal{K}_{\nu_{lm}}(\cdot)$ is the modified Bessel function of the second kind with a positive roughness parameter ν_{lm} and a nonnegative range parameter γ_{lm} for $l = 1, \dots, d$ and $m = 1, \dots, p$. The Matérn kernel contains a wide range of different kernel functions. In particular, when $\nu_{lm} = 1/2$, the Matérn kernel becomes the exponential kernel, $K_l(x_{am}, x_{bm}) = \exp(-|x_{am} - x_{bm}|/\gamma_{lm})$, and the corresponding factor process is the Ornstein-Uhlenbeck process, which is a continuous autoregressive process with order 1. When $\nu_{lm} \rightarrow \infty$, the Matérn kernel becomes the Gaussian kernel, $K_l(x_{am}, x_{bm}) = \exp(-|x_{am} - x_{bm}|^2/\gamma_{lm}^2)$, where the factor process is infinitely differentiable. The Matérn kernel has a closed-form expression when $(2\nu_{lm} + 1)/2 \in \mathbb{N}$. E.g., the Matérn kernel with $\nu_{lm} = 5/2$ has the following form

$$K_{lm}(x_{am}, x_{bm}) = \left(1 + \frac{\sqrt{5}|x_{am} - x_{bm}|}{\gamma_{lm}} + \frac{5|x_{am} - x_{bm}|^2}{3\gamma_{lm}^2} \right) \exp \left(-\frac{\sqrt{5}|x_{am} - x_{bm}|}{\gamma_{lm}} \right), \quad (12)$$

for any inputs \mathbf{x}_a and \mathbf{x}_b with $l = 1, \dots, d$ and $m = 1, \dots, p$.

We denote $\tau_l := \frac{\sigma_l^2}{\sigma_0^2}$ as the variance of the signal to noise ratio (SNR) for the l th factor process, as a transformation of σ_l^2 in (10). Further let $\tilde{\Sigma}_l = \Sigma_l/\sigma_0^2$ for $l = 1, \dots, d$. The following lemma gives the maximum marginal likelihood estimator for the parameters in model (1), by integrating out the factor processes.

Lemma 2. *Under Assumption 1, after marginalizing out \mathbf{Z} and plugging $\hat{\mathbf{A}} = [\hat{\mathbf{a}}_1, \dots, \hat{\mathbf{a}}_d]$, the maximum likelihood estimator of σ_0^2 is*

$$\hat{\sigma}_0^2 = \frac{\hat{S}^2}{nk}, \quad (13)$$

where $\hat{S}^2 = \text{tr}(\mathbf{Y}^T \mathbf{Y}) - \sum_{l=1}^d \hat{\mathbf{a}}_l^T \mathbf{Y} (\tilde{\Sigma}_l^{-1} + \mathbf{I}_n)^{-1} \mathbf{Y}^T \hat{\mathbf{a}}_l$; ignoring the constants, the likelihood of $\boldsymbol{\tau} = (\tau_1, \dots, \tau_d)$ and $\boldsymbol{\gamma} = (\gamma_1, \dots, \gamma_d)$ is

$$L(\boldsymbol{\tau}, \boldsymbol{\gamma} \mid \mathbf{Y}, \hat{\mathbf{A}}, \hat{\sigma}_0^2) \propto \left\{ \prod_{l=1}^d |\tilde{\Sigma}_l + \mathbf{I}_n|^{-1/2} \right\} |\hat{S}^2|^{-nd/2}. \quad (14)$$

Since there is no closed-form expression for the parameters $(\boldsymbol{\tau}, \boldsymbol{\gamma})$ in the kernels, one often numerically maximizes the Equation (14) to estimate these parameters

$$(\hat{\boldsymbol{\tau}}, \hat{\boldsymbol{\gamma}}) := \underset{(\boldsymbol{\tau}, \boldsymbol{\gamma})}{\operatorname{argmax}} L(\boldsymbol{\tau}, \boldsymbol{\gamma} \mid \mathbf{Y}, \hat{\mathbf{A}}, \hat{\sigma}_0^2). \quad (15)$$

After obtaining $\hat{\sigma}_0^2$ and $\hat{\boldsymbol{\tau}}$ from (13) and (15), respectively, we transform the expressions back to get the estimator of σ_l^2 as

$$\hat{\sigma}_l^2 = \hat{\tau}_l \hat{\sigma}_0^2,$$

for $l = 1, \dots, d$. Since both the estimator of $\hat{\sigma}_0^2$ and $\hat{\mathbf{A}}$ in Theorem 1 and 2 can be expressed as a function of $(\boldsymbol{\tau}, \boldsymbol{\gamma})$, in each iteration, one can use the Newton's method (Nocedal, 1980) to find $(\boldsymbol{\tau}, \boldsymbol{\gamma})$ based on the likelihood in (14), plugging the the estimator of $\hat{\sigma}_0^2$ and $\hat{\mathbf{A}}$. The maximum likelihood estimator of $(\hat{\boldsymbol{\tau}}, \hat{\boldsymbol{\gamma}})$ is not robust when the number of the observations is small to moderate, in a sense that the estimated range parameters can be very small. This might be unsatisfying in certain applications, such as emulating computationally expensive computer models (Oakley (1999)). An alternative way is to replace the maximum profile likelihood estimation by the maximum marginal posterior estimation using the reference prior with a robust parameterization. We refer to Gu et al. (2018b) for the theoretical properties of this estimator and an R package is available on CRAN (Gu et al. (2018a)). In this work, we implement all numerical studies by maximizing the likelihood in (15) to obtain $(\hat{\boldsymbol{\tau}}, \hat{\boldsymbol{\gamma}})$.

We have a few remarks regarding the expressions in Lemma 2. First of all, consider the first term at the right hand side of \hat{S}^2 . As each row of \mathbf{Y} has a zero mean, denote

$$\mathbf{S}_0^2 := \frac{\mathbf{Y}\mathbf{Y}^T}{n} = \frac{\sum_{i=1}^n \mathbf{y}(\mathbf{x}_i)\mathbf{y}(\mathbf{x}_i)^T}{n},$$

the sample covariance matrix for $\mathbf{y}(\mathbf{x}_i)$. One has $\text{tr}(\mathbf{Y}\mathbf{Y}^T) = n \sum_{i=1}^k \lambda_{0i}$ where λ_{0i} is the i th eigenvalues of \mathbf{S}_0^2 . The second term at the right hand side of \hat{S}^2 is the variance explained by the projection. In particular, when the conditions in Theorem 1 hold, i.e. $\boldsymbol{\Sigma}_1 = \dots = \boldsymbol{\Sigma}_d$, one has $\sum_{l=1}^d \hat{\mathbf{a}}_l^T \mathbf{Y} (\hat{\boldsymbol{\Sigma}}_l^{-1} + \mathbf{I}_n)^{-1} \mathbf{Y}^T \hat{\mathbf{a}}_l = n \sum_{l=1}^d \hat{\lambda}_l$ where $\hat{\lambda}_l$ is the l th largest eigenvalues of $\mathbf{Y}(\sigma_0^2 \boldsymbol{\Sigma}^{-1} + \mathbf{I}_n)^{-1} \mathbf{Y} / n$. The estimation of the noise is then the average variance lost in the projection. Note that the projection in the GPPCA takes into account the correlation of the factor processes, whereas the projection in the PPCA assumes the independent factors. This difference makes the GPPCA more accurate in estimating the subspace of the factor loading matrix when the factors are correlated, shown in various numerical studies in Section 4.

Secondly, although the model in (1) is regarded as a nonseparable model (Fricker et al. (2013)), the computational complexity of our algorithm, is the same as the separable model (Gu and Berger (2016); Conti and O'Hagan (2010)). Instead of inverting an $nk \times nk$ covariance matrix, the expression of the maximum likelihood estimator in Lemma 2 allows us to proceed in the same way with that the covariance matrix for each factor has the size of $n \times n$. The number of computational operations of the likelihood is typically $\max(O(dn^3), O(dkn^2))$, which is much small than the $O(n^3k^3)$ for inverting an $nk \times nk$ covariance matrix, because one often has $d \ll k$. When the input is one-dimensional and the Matérn kernel in (11) is used, the computational operations are only $O(dkn)$ for computing the likelihood in (14) without any approximation (see e.g. Hartikainen and Sarkka (2010); Gu and Xu (2017)).

Furthermore, the GPPCA provides a data-driven method for quantifying the correlation among the factor processes via the range parameters in the kernel functions. By taking the correlation into account, the estimator of σ_0^2 is found to be more accurate in numerical studies. In comparison, the variance parameter of the noise is often underestimated by the PPCA when the factors are correlated. Numerous examples regarding this finding will be discussed in Sections 3 and 4.

Given the parameter estimates, we can also obtain the predictive distribution for the outputs. Let $\hat{K}_l(\cdot, \cdot)$ be the l th kernel function after plugging the estimator $(\hat{\sigma}_l^2, \hat{\gamma}_l)$ and let

$\hat{\Sigma}_l$ be the estimator of the covariance matrix for the l th factor, where the (i, j) element of $\hat{\Sigma}_l$ is $\hat{K}_l(\mathbf{x}_i, \mathbf{x}_j)$, with $1 \leq i, j \leq n$ and $l = 1, \dots, d$. We have the following predictive distribution for the outputs at any given input.

Theorem 3. *Under the Assumption 1, for any \mathbf{x}^* , one has*

$$\mathbf{Y}(\mathbf{x}^*) \mid \mathbf{Y}, \hat{\mathbf{A}}, \hat{\gamma}, \hat{\sigma}^2, \hat{\sigma}_0^2 \sim \text{MN} \left(\hat{\boldsymbol{\mu}}^*(\mathbf{x}^*), \hat{\boldsymbol{\Sigma}}^*(\mathbf{x}^*) \right).$$

Here

$$\hat{\boldsymbol{\mu}}^*(\mathbf{x}^*) = \hat{\mathbf{A}}\hat{\mathbf{z}}(\mathbf{x}^*), \quad (16)$$

where $\hat{\mathbf{z}}(\mathbf{x}^*) = (\hat{z}_1(\mathbf{x}^*), \dots, \hat{z}_d(\mathbf{x}^*))^T$, with $\hat{z}_l(\mathbf{x}^*) = \hat{\Sigma}_l(\mathbf{x}^*)(\hat{\Sigma}_l + \hat{\sigma}_0^2 \mathbf{I}_n)^{-1} \mathbf{Y}^T \hat{\mathbf{a}}_l$, $\hat{\Sigma}_l(\mathbf{x}^*) = (\hat{K}_l(\mathbf{x}_1, \mathbf{x}^*), \dots, \hat{K}_l(\mathbf{x}_n, \mathbf{x}^*))$ for $l = 1, \dots, d$, and

$$\hat{\boldsymbol{\Sigma}}^*(\mathbf{x}^*) = \hat{\sigma}_0^2(\mathbf{I}_k + \hat{\mathbf{A}}\hat{\mathbf{D}}(\mathbf{x}^*)\hat{\mathbf{A}}^T). \quad (17)$$

In (17), $\hat{\mathbf{D}}(\mathbf{x}^*)$ is a diagonal matrix, where the l th diagonal term, denoted as $\hat{D}_l(\mathbf{x}^*)$, has the following expression

$$\hat{D}_l(\mathbf{x}^*) = \frac{1}{\sigma_0^2} \left(\hat{K}(\mathbf{x}^*, \mathbf{x}^*) - \hat{\Sigma}_l(\mathbf{x}^*)^T \left(\hat{\Sigma}_l + \hat{\sigma}_0^2 \mathbf{I}_n \right)^{-1} \hat{\Sigma}_l(\mathbf{x}^*) \right),$$

for $l = 1, \dots, d$.

In practice, the posterior distribution of the $d \times n$ factor matrix \mathbf{Z} is often not identifiable, whereas the posterior of \mathbf{AZ} , given in following Corollary 1, is identifiable.

Corollary 1 (Posterior distribution of \mathbf{AZ}). *Under the Assumption (1), the posterior of \mathbf{AZ} is*

$$(\mathbf{AZ} \mid \mathbf{Y}, \hat{\mathbf{A}}, \hat{\gamma}, \hat{\sigma}^2, \hat{\sigma}_0^2) \sim \text{MN} \left(\hat{\mathbf{A}}\hat{\mathbf{Z}}, \hat{\sigma}_0^2 \sum_{l=1}^d \hat{\mathbf{D}}_l \otimes \hat{\mathbf{a}}_l \hat{\mathbf{a}}_l^T \right),$$

where $\hat{\mathbf{Z}} = (\hat{\mathbf{Z}}_1^T, \dots, \hat{\mathbf{Z}}_d^T)^T$, $\hat{\mathbf{Z}}_l^T = \hat{\Sigma}_l(\hat{\Sigma}_l + \hat{\sigma}_0^2 \mathbf{I}_n)^{-1} \mathbf{Y}^T \hat{\mathbf{a}}_l$, and $\hat{\mathbf{D}}_l = \left(\sigma_0^2 \hat{\Sigma}_l^{-1} + \mathbf{I}_n \right)^{-1}$, for $l = 1, \dots, d$.

The Corollary 1 is a direct consequence of Theorem 3, so the proof is omitted. Note that the uncertainty of the parameters and the loading factors are not taken into consideration for predictive distribution of $\mathbf{Y}(\mathbf{x}^*)$ in Theorem 3 and the posterior distribution of \mathbf{AZ} in Corollary 1, because of the use of the plug-in estimator of $(\mathbf{A}, \sigma_0^2, \sigma^2, \gamma)$. The resulting posterior credible interval may be narrower than it should be when the sample size is small to moderate. The uncertainty of \mathbf{A} and other model parameters can be obtained by a full Bayesian analysis with a prior for these parameters, and it is a possible future direction based on the closed-form marginal likelihood we derived.

3 Comparison to other approaches

We compare our method to various other frequently used approaches in this section. First of all, the MLE of the factor loading matrix \mathbf{A} under the Assumption 1 is $\mathbf{U}_0 \mathbf{R}$, where \mathbf{U}_0

is the first d ordered eigenvectors of $\mathbf{S}_0^2 = \mathbf{Y}\mathbf{Y}^T/n$ and \mathbf{R} is an arbitrary orthogonal rotation matrix. This approach is a version of principal component analysis, widely applied in the literature for the inference of the latent factor model. For example, Bai and Ng (2002); Bai (2003) assume $\mathbf{A}^T\mathbf{A}/k = \mathbf{I}_d$ and estimate \mathbf{A} by $\sqrt{k}\mathbf{U}_0$ in modeling high-dimensional time series. Compared to the MLE, we model the latent factor processes via the Gaussian processes (GPs), in which the uncertainty has been taken into consideration by the proposed marginal maximum likelihood estimator of \mathbf{A} in Theorem 1 and Theorem 2. Another version of the PCA takes the singular value decomposition (SVD) of $\mathbf{Y} = \mathbf{U}_0\mathbf{\Lambda}_0\mathbf{V}_0^T$ and estimates \mathbf{A} by $\mathbf{U}_0\mathbf{\Lambda}_0/\sqrt{n}$ (Higdon et al., 2008).

The PCA approach has been widely explored in the literature and the principal axes of the PCA is the same as the PPCA, which estimates the factor loading matrix by the maximum marginal likelihood estimator, after marginalizing out the independent factors. More specifically, assuming independent normally distributed factors \mathbf{Z} , Tipping and Bishop (1999) shown that the maximum marginal likelihood estimator for \mathbf{A} after marginalizing out \mathbf{Z} is $\mathbf{U}_0(\mathbf{D}_0 - \sigma_0^2\mathbf{I}_n)\mathbf{R}$, where \mathbf{D}_0 is a diagonal matrix whose l th diagonal term is the l th largest eigenvalues of \mathbf{S}_0^2 and \mathbf{R} is an arbitrary orthogonal rotation matrix.

The PPCA gives a full probabilistic model of the PCA by modeling \mathbf{Z} via independent normal distributions. However, when each output is correlated at different inputs, modeling the factor processes as independent normal distributions along with the latent factor model in (1) may not be a good sampling model. In comparison, the factors are allowed to be correlated in the GPPCA, which is a more flexible model for the correlated output data. Therefore, our approach can be viewed as a generalized approach of the PPCA for the correlated data, where the maximum marginal likelihood estimator for \mathbf{A} is derived based on the assumption that each row of \mathbf{Z} is a multivariate normal distribution. We illustrate the difference between the GPPCA and PCA using the following Example 1.

Example 1. *The data is sampled from the model (1) with the shared covariance matrix $\mathbf{\Sigma}_1 = \mathbf{\Sigma}_2 = \mathbf{\Sigma}$, where x is equally spaced from 1 to n and the kernel function is assumed to follow (12) with $\gamma = 100$ and $\sigma^2 = 1$. We choose $k = 2$, $d = 1$ and $n = 100$. Two scenarios are implemented with $\sigma_0^2 = 0.01$ and $\sigma_0^2 = 1$, respectively. The parameters $(\sigma_0^2, \sigma^2, \gamma)$ are assumed to be unknown and estimated from the data.*

Note the linear subspace spanned from the column space of estimated loading matrix by the PCA or PPCA is the same, which is $\mathcal{M}(\mathbf{U}_0)$, even though the form of these estimators are slightly different. Thus we only compare the GPPCA to the PCA in Figure 1 where \mathbf{A} is a two-dimensional vector generated from a uniform distribution on the Stiefel manifold (Hoff, 2018). The signal to noise ratio (SNR) is $\tau = 10^2$ and $\tau = 1$ for the upper and lower panels in Figure 1, respectively.

When the SNR is large, two rows of the outputs are strongly correlated, as shown in the upper left panel in Figure 1, with the empirical correlation being around 0.66 between two rows of the output \mathbf{Y} . The estimated subspaces by the PCA and GPPCA both match the true \mathbf{A} equally well in this scenario, shown in the upper right panel. When the variance of the noise gets large, the outputs are no longer very correlated. E.g. the empirical correlation between two simulated output variables is only around -0.18 . As a result, the angle between the estimated subspace and the column space of \mathbf{A} by the PCA is large, shown in the right lower panel.

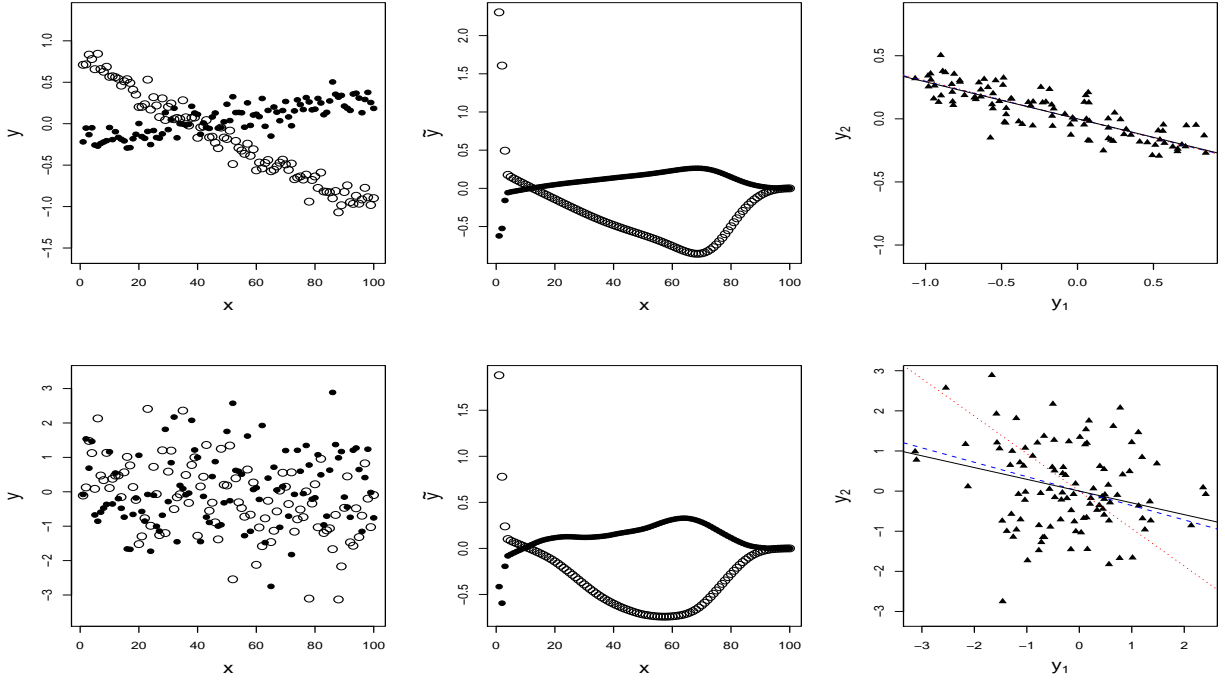


Figure 1: Estimation of the factor loading matrix by the PCA and GPPCA for Example 1 with the variance of the noise being $\sigma_0^2 = 0.01$ and $\sigma_0^2 = 1$, graphed in the upper panels and lower panels, respectively. The circles and dots are the first and second rows of \mathbf{Y} in the left panel, and of the transformed output $\tilde{\mathbf{Y}} = \mathbf{Y}\mathbf{L}$ in the middle panels, where \mathbf{L} is the left triangle matrix of the Cholesky decomposition $(\sigma_0^2\mathbf{\Sigma}^{-1} + \mathbf{I}_n)^{-1}$. In the right panels, the black solid lines, blue dash lines and red dotted lines are the subspace of \mathbf{A} , the first eigenvector of \mathbf{U}_0 and the first eigenvector of \mathbf{G} in Theorem 1, respectively, with the black triangles being the outputs. The black, blue and red lines almost overlap in the upper right panel.

The GPPCA by Theorem 1 essentially transforms the output by $\tilde{\mathbf{Y}} = \mathbf{Y}\mathbf{L}$, graphed in the middle panels, where \mathbf{L} is the left triangle matrix of the Cholesky decomposition for $(\sigma_0^2\mathbf{\Sigma}^{-1} + \mathbf{I}_n)^{-1}$. The two rows of the transformed outputs are strongly correlated, shown in the middle panels. The empirical correlation between two rows of the transformed outputs graphed in the lower panel is about -0.91 , even though the variance of the noise is as large as the variance of the signal. By Theorem 1, the subspace by the GPPCA is equivalent to the first eigenvector of the transformed output for this example, and it is graphed as the blue dashed curves in the right panels. The estimated subspace by the GPPCA is very close to the truth in both scenarios, even when the variance of the noise is large in the second scenario.

For PCA, the mean of the outputs is typically estimated by the maximum likelihood estimator $\hat{\mathbf{A}}_{pca}\hat{\mathbf{A}}_{pca}^T\mathbf{Y}$, where $\hat{\mathbf{A}}_{pca} = \mathbf{U}_0$ (Bai and Ng, 2002). In Figure 2, the PCA estimation of the mean for Example 1 is graphed as the red curves and the posterior mean of the output in the GPPCA in Corollary 1 is graphed as the blue curves. The PCA approach underestimates the variance of the noise, and the error of the estimation is large as a conse-

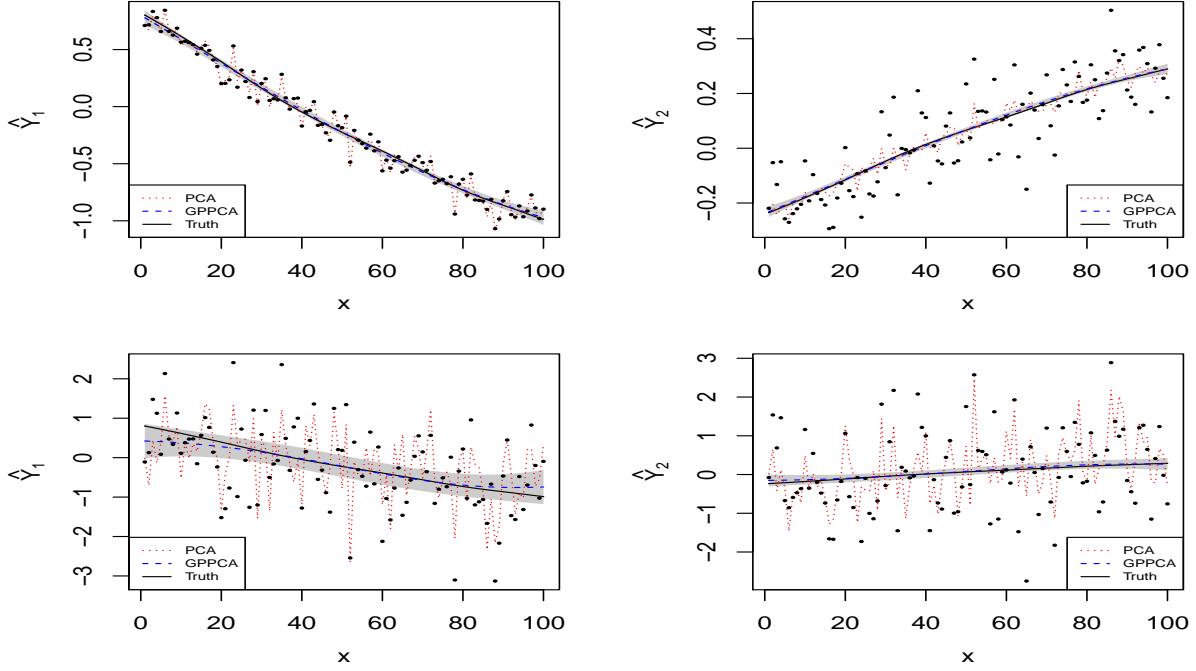


Figure 2: Estimation of the mean of the output \mathbf{Y} for Example 1 with the variance of the noise being $\sigma_0^2 = 0.01$ and $\sigma_0^2 = 1$, graphed in the upper panels and lower panels, respectively. The first row and second row of \mathbf{Y} are graphed as the black curves at the left panels and right panels, respectively. The red dotted curves and the blue dashed curves are the prediction by the PCA and GPPCA, respectively. The grey region is the 95% posterior credible interval from GPPCA. The black curves, blue curves and grey regions almost overlap in the upper panels.

quence. In comparison, the estimated mean of the output by the GPPCA is more accurate, as the correlation in each output variable is properly modeled through the GPs of the latent factors.

Note we constrain \mathbf{A} to satisfy $\mathbf{A}^T \mathbf{A} = \mathbf{I}_d$ to simulate the examples shown in Figure 1. In practice, we found this only affects the estimation of the variance parameter σ_l^2 in the kernel, $l = 1, \dots, d$, because the meaning of this parameter changes.

Some other approaches appeared in estimating \mathbf{A} in the latent factor model of the high-dimensional time series. E.g. Lam et al. (2011); Lam and Yao (2012) estimate the factor loading matrix of model (1) by $\hat{\mathbf{A}}_{LY} := \sum_{q=1}^{q_0} \hat{\Sigma}_y(q) \hat{\Sigma}_y^T(q)$, where $\hat{\Sigma}_y(q)$ is the $k \times k$ sample covariance at lag q of the output and q_0 is fixed to be a small positive integer. This approach is sensible, because $\mathcal{M}(\mathbf{A})$ is shown to be spanned from $\sum_{q=1}^{q_0} \Sigma_y(q) \Sigma_y^T(q)$ under some reasonable assumptions, where $\Sigma_y(q)$ is the underlying lag- q covariance of the outputs. It is also suggested in Lam and Yao (2012) to estimate the latent factor by $\hat{\mathbf{Z}}_{LY} = \hat{\mathbf{A}}_{LY}^T \mathbf{Y}$, meaning that the mean of the output is estimated by $\hat{\mathbf{A}}_{LY} \hat{\mathbf{Z}}_{LY} = \hat{\mathbf{A}}_{LY} \hat{\mathbf{A}}_{LY}^T \mathbf{Y}$. This estimator and the PCA are both included for comparison in Section 4.

4 Numerical results

In this section, we numerically compare different approaches studied before. We use several criteria to examine the estimation. The first criterion is the last principal angle between the estimated subspace $\mathcal{M}(\hat{\mathbf{A}})$ and the true subspace $\mathcal{M}(\mathbf{A})$. Let $0 \leq \phi_1 \leq \dots \leq \phi_d \leq \pi/2$ be the principal angles between $\mathcal{M}(\mathbf{A})$ and $\mathcal{M}(\hat{\mathbf{A}})$, recursively defined by

$$\phi_i = \arccos \left(\max_{\mathbf{a} \in \mathcal{M}(\mathbf{A}), \hat{\mathbf{a}} \in \mathcal{M}(\hat{\mathbf{A}})} |\mathbf{a}^T \hat{\mathbf{a}}| \right) = \arccos(|\mathbf{a}_i^T \hat{\mathbf{a}}_i|),$$

subject to

$$\|\mathbf{a}\| = \|\hat{\mathbf{a}}\| = 1, \mathbf{a}^T \mathbf{a}_i = 0, \hat{\mathbf{a}}^T \hat{\mathbf{a}}_i = 0, i = 1, \dots, d-1.$$

The last principal angle is ϕ_d , which quantifies how close two linear subspaces are. When two subspaces are identical, all principal angles are zero. The principal angle can be calculated through the singular value decomposition of $\hat{\mathbf{A}}^T \mathbf{A}$. We refer to Björck and Golub (1973); Reynkens (2018) for the numerical algorithm of calculating the last principal angle.

We numerically compare four approaches for estimating \mathbf{A} . The first approach is the PCA, which estimates \mathbf{A} by \mathbf{U}_0 , where \mathbf{U}_0 is the first d eigenvectors of $\mathbf{Y}\mathbf{Y}^T/n$. Note the other version of the PCA and the PPCA all have the same last principal angle between the estimated subspace of \mathbf{A} and the true subspace of \mathbf{A} , so the results are omitted. The estimation of the GPPCA is the second approach. When the covariance of the factor processes is the same, the closed-form expression of the estimator of the factor loading matrix is given in Theorem 1. When the covariance of the factor processes is different, we implement the optimization algorithm in Wen and Yin (2013) that preserves the orthogonal constraints to obtain the maximum marginal likelihood estimation of the factor loading matrix in Theorem 2. The parameters $(\gamma, \tau, \sigma_0^2)$ are treated unknown and estimated by maximizing the marginal likelihood after integrating out \mathbf{Z} , given in Lemma 2. The third approach, denoted as LY1, estimates \mathbf{A} by $\hat{\Sigma}_y(1)\hat{\Sigma}_y^T(1)$, where $\hat{\Sigma}_y(1)$ is the sample covariance of the output at lag 1 and the fourth approach, denoted as LY5, estimates \mathbf{A} by $\sum_{q=1}^{q_0} \hat{\Sigma}_y(q)\hat{\Sigma}_y^T(q)$ with $q_0 = 5$, used in Lam and Yao (2012) and Lam et al. (2011), respectively.

We also compare the performance of different approaches by the average mean squared errors (AvgMSE) in predicting the mean of the output over N experiments as follows

$$\text{AvgMSE} = \sum_{l=1}^N \sum_{j=1}^n \sum_{i=1}^k \frac{(\hat{Y}_{i,j}^{(l)} - \mathbb{E}[Y_{i,j}^{(l)}])^2}{knN}, \quad (18)$$

where $\mathbb{E}[Y_{i,j}^{(l)}]$ is the (i, j) element of the mean of the output matrix at the l th experiment, and $\hat{Y}_{i,j}^{(l)}$ is the estimation. As discussed in (4), the estimation of the mean of the output matrix by the PCA, LY1 and LY5 is $\hat{\mathbf{A}}\hat{\mathbf{A}}^T\mathbf{Y}$, where $\hat{\mathbf{A}}$ is the estimated factor loading matrix in each approach (Bai and Ng (2002); Lam et al. (2011); Lam and Yao (2012)). In GPPCA, we use the posterior mean of \mathbf{AZ} given in Corollary 1 to estimate mean of the output matrix.

Both the correctly specified model and misspecified model are used to sample data in the numerical comparison. In Section 4.1, we assume \mathbf{A} is sampled from the uniform distribution on the Stiefel manifold (Hoff (2018)), and the kernels are correctly specified with unknown

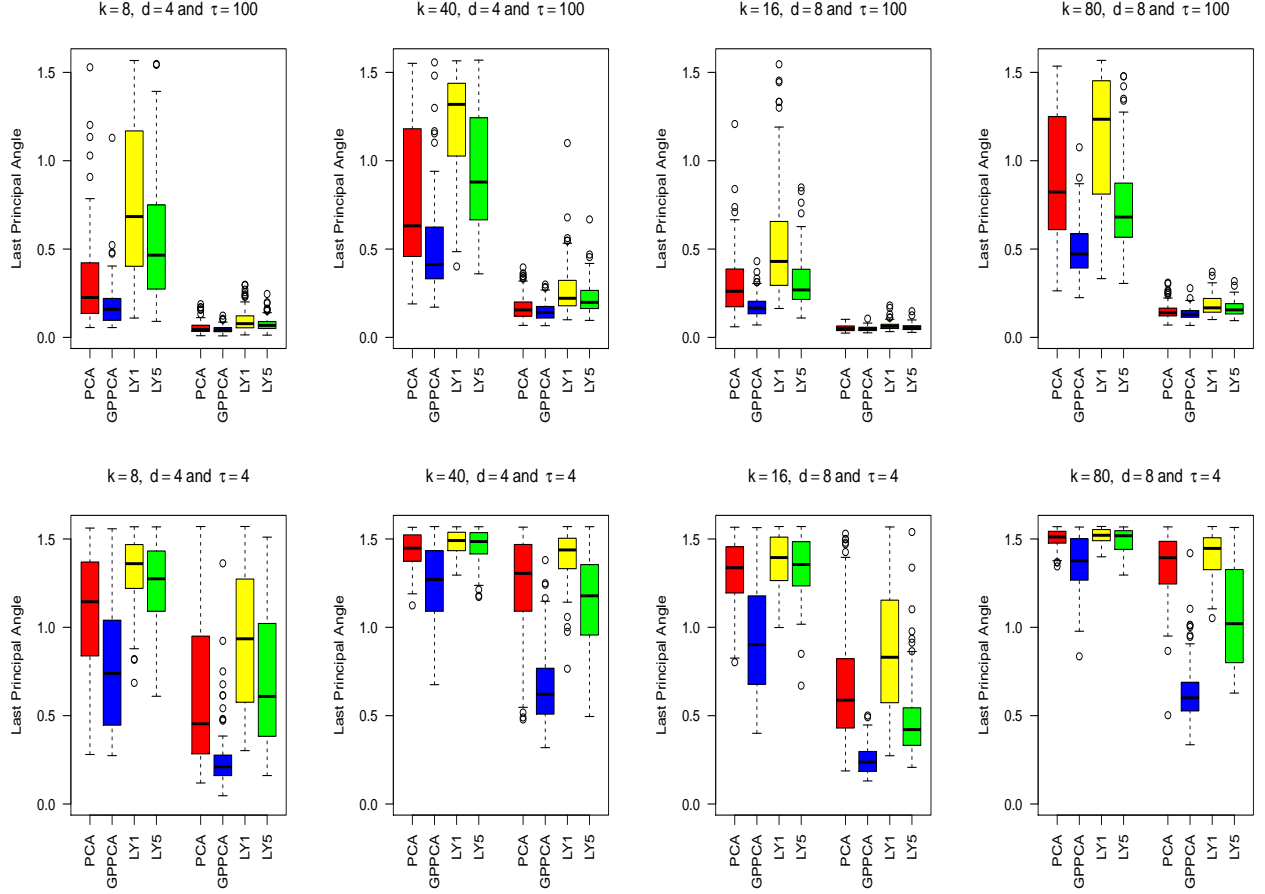


Figure 3: The last principal angle between the true subspace of the factor loading matrix and the estimation from the four approaches for Example 2 (ranging from $[0, \pi/2]$, the smaller the better). In the first row, the number of the observations of each output variable is assumed to be $n = 200$ and $n = 400$ for the left four boxplots and right four boxplots in each panel, respectively. In the second row, the number of observations is assumed to be $n = 500$ and $n = 1000$ for the left four boxplots and right four boxplots in each panel, respectively.

parameters. In Section 4.2, we compare the performance of different approaches due to three different types of misspecification in the model.

4.1 Correctly specified model

We first compare the performance using a simple example where the covariance of the factor process is shared.

Example 2 (Factors with the same covariance matrix). *The data is sampled from model (1) with $\Sigma_1 = \dots = \Sigma_n = \Sigma$ where x is equally spaced from 1 to n and the kernel function in (12) is used with $\gamma = 100$ and $\sigma^2 = 1$. In each scenario, we simulate the data from 16 different combinations of σ_0^2 , k , d and n . We repeat $N = 100$ times for each scenario. The parameters $(\sigma_0^2, \sigma^2, \gamma)$ are treated as unknown and estimated from the data.*

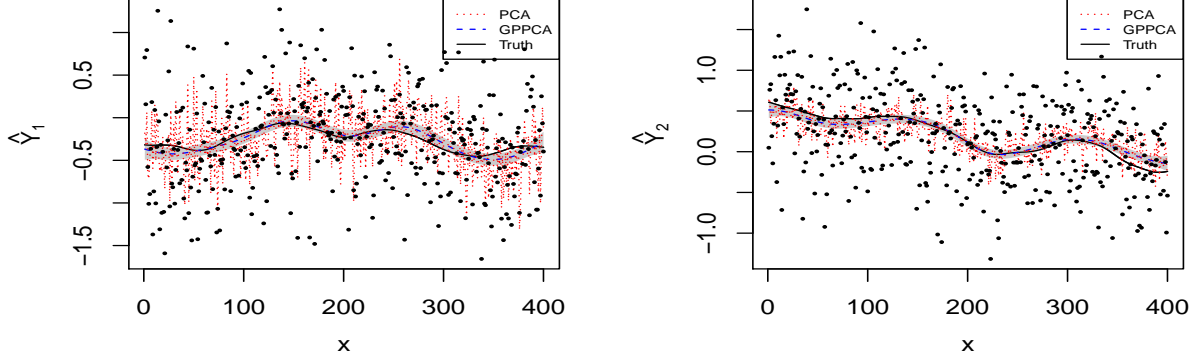


Figure 4: Prediction of the mean of the first two output variables in one experiment with $k = 8$, $d = 4$, $n = 400$ and $\tau = 4$. The observations are plotted as black circles and the truth is graphed as the black curves. The estimation by PCA and GPPCA is graphed as the red dotted curves and blue dashed curves, respectively. The shaded area is the 95% posterior credible interval by the GPPCA.

The last principal angle between the true subspace $\mathcal{M}(\mathbf{A})$ and estimated subspace $\mathcal{M}(\hat{\mathbf{A}})$ at different settings of Example 1 is graphed in Figure 3, with the red, blue, yellow and green boxplots being the ones by the PCA, GPPCA, LY1 and LY5. The right 4 boxplots have the sample size twice as large as the left 4 boxplots in each panel.

Since the covariance of the factor processes is the same in Example 2, the estimator of \mathbf{A} by the GPPCA has a closed-form solution given in Theorem 1. For all 16 different scenarios of Example 2, the GPPCA outperforms the other three methods in terms of having the smallest last principal angle between $\mathcal{M}(\mathbf{A})$ and $\mathcal{M}(\hat{\mathbf{A}})$. Both PCA and GPPCA can be viewed as a type of the maximum likelihood approaches under the assumption of the orthonormal columns of the factor loading matrix. The difference is that the estimator of \mathbf{A} by the GPPCA maximizes the marginal likelihood after integrating out the factor processes, whereas the PCA maximizes the likelihood without modeling the factor processes. The principal axes by the PCA is the same as the PPCA which assumes the factors are independently distributed. As discussed before, the model with independent factors, however, is not a sensible sampling model for the correlated data, such as the multiple time series or multivariate spatial processes.

The performance of all methods improves when the sample size increases or the SNR increases, shown in Figure 3. The LY5 estimator (Lam et al. (2011)) seems to perform slightly better than the PCA when the SNR is smaller. This method is sensible because the factor loading space $\mathcal{M}(\mathbf{A})$ is spanned by the eigenvectors of $\mathbf{M} := \sum_{i=1}^{q_0} \Sigma_y(q) \Sigma_y^T(q)$ under some conditions. However, this may not be the unique way to represent the subspace of the factor loading matrix. Thus the estimator based on this argument may not be as efficient as the maximum marginal likelihood approach by the GPPCA, shown in Figure 3.

The AvgMSE of the different approaches for Example 2 is shown in Table 1. The mean squared error of the estimation by the GPPCA is typically a digit or two smaller than the

$d = 4$ and $\tau = 100$	k=8		k=40	
	$n = 200$	$n = 400$	$n = 200$	$n = 400$
PCA	5.3×10^{-3}	5.1×10^{-3}	1.4×10^{-3}	1.1×10^{-3}
GPPCA	3.3×10^{-4}	2.6×10^{-4}	2.2×10^{-4}	1.3×10^{-4}
LY1	4.6×10^{-2}	5.8×10^{-3}	1.5×10^{-2}	2.1×10^{-3}
LY5	3.2×10^{-2}	5.5×10^{-3}	1.1×10^{-2}	1.8×10^{-3}
$d = 8$ and $\tau = 100$	k=16		k=80	
	$n = 500$	$n = 1000$	$n = 500$	$n = 1000$
PCA	5.2×10^{-3}	5.0×10^{-3}	1.3×10^{-3}	1.1×10^{-3}
GPPCA	2.9×10^{-4}	2.4×10^{-4}	1.9×10^{-4}	1.1×10^{-4}
LY1	1.4×10^{-2}	5.1×10^{-3}	5.4×10^{-3}	1.2×10^{-3}
LY5	8.8×10^{-3}	5.1×10^{-3}	3.9×10^{-3}	1.2×10^{-3}
$d = 4$ and $\tau = 4$	k=8		k=40	
	$n = 200$	$n = 400$	$n = 200$	$n = 400$
PCA	1.4×10^{-1}	1.3×10^{-1}	4.2×10^{-2}	3.4×10^{-2}
GPPCA	5.8×10^{-3}	4.4×10^{-3}	5.3×10^{-3}	3.0×10^{-3}
LY1	2.2×10^{-1}	1.7×10^{-1}	7.2×10^{-2}	6.4×10^{-2}
LY5	2.2×10^{-1}	1.5×10^{-1}	4.8×10^{-2}	4.1×10^{-2}
$d = 8$ and $\tau = 4$	k=16		k=80	
	$n = 500$	$n = 1000$	$n = 500$	$n = 1000$
PCA	1.4×10^{-1}	1.3×10^{-1}	3.9×10^{-2}	3.2×10^{-2}
GPPCA	5.1×10^{-3}	3.9×10^{-3}	4.3×10^{-3}	2.4×10^{-3}
LY1	1.8×10^{-1}	1.4×10^{-1}	5.1×10^{-2}	3.4×10^{-2}
LY5	1.7×10^{-1}	1.3×10^{-1}	4.6×10^{-2}	3.1×10^{-2}

Table 1: AvgMSE for Example 2.

ones by the other approaches. This is because the correlation of the factor processes in the GPPCA is properly modeled, and the kernel parameters are estimated based on the maximum marginal likelihood estimation.

We plot the estimated first two rows of the mean of the output in one experiment from the Example 2 in Figure 4. The estimation of the GPPCA approach is graphed as the blue dashed curves, which is very close to the truth, graphed as the black curves, whereas the estimation by the PCA is graphed as the red dotted curves, which are less smooth and less accurate in predicting the mean of the outputs, because of the noise in the data. The estimators by LY1 and LY5 are similar to those of PCA so we omit them in Figure 4. The problem of the PCA is that the estimated subspace of the factor loading matrix is equivalent to the one of the PPCA which assumes that the factors are independently distributed. This independence assumption makes the likelihood too concentrated. Hence the variance of the noise is underestimated as indicated by the red curves in Figure 4.

In comparison, the variance of the noise estimated by the GPPCA is closer to the truth, which makes posterior mean of the output closer to the truth. The 95% posterior credible interval by the GPPCA is also close to the 95% nominal level when the sample size is large. When the sample size is small, since the uncertainty of estimating \mathbf{A} and other parameters

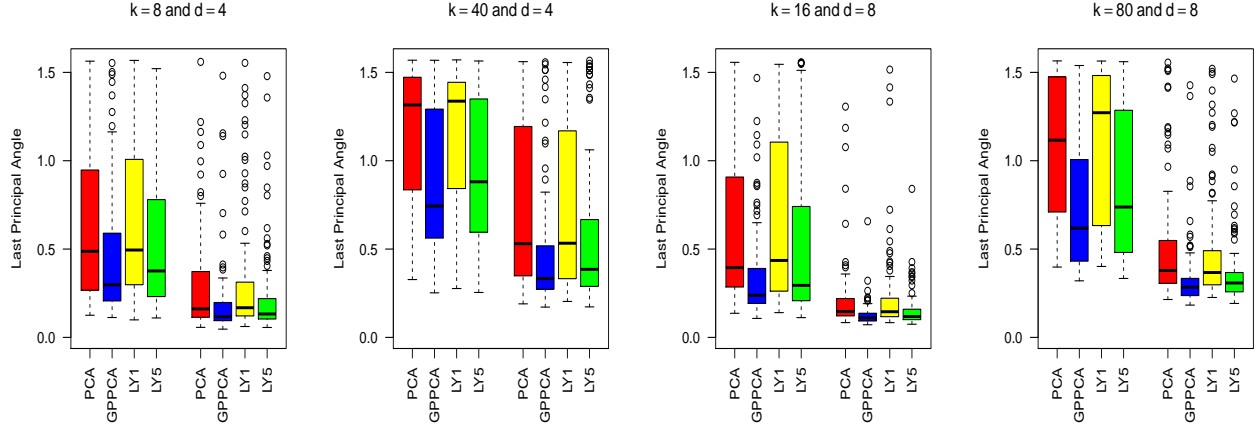


Figure 5: The last principal angle between the true subspace and the estimated subspace of the four approaches for Example 3. The number of observations of each output variable is $n = 200$ and $n = 400$ for left 4 boxplots and right 4 boxplots in the first 2 panels, respectively. The number of observations is $n = 500$ and $n = 1000$ for left 4 boxplots and right 4 boxplots in the last 2 panels, respectively.

are not taken into account in the prediction, the 95% interval tends to be narrower than it should be.

Note the improvement of the GPPCA in estimating the mean of the output comes from modeling the correlation in the factor processes. An alternative estimator of the mean of the output is to fit independent Gaussian processes for each row of the output as in the nonparametric regression. We will numerically compare with this approach in Example 5.

Example 3 (Factors with different covariance matrices). *The data is sampled from model (1) where x is equally spaced from 1 to n . The variance of the noise is $\sigma_0^2 = 0.25$ and the kernel function is assumed to follow from (12) with $\sigma^2 = 1$. The range parameter γ of each factor is uniformly sampled from $[10, 10^3]$ in each experiment. In each scenario, we simulate the data from 8 different combinations of k , d and n . We repeat $N = 100$ times for each scenario. The parameters in the kernels and the variance of the noise are treated as unknown and estimated from the data.*

The last principal angle between $\mathcal{M}(\mathbf{A})$ and $\mathcal{M}(\hat{\mathbf{A}})$ and the AvgMSE in estimating the mean of the output matrix by different approaches for Example 3 is given in Figure 5 and Table 2, respectively. The estimation by the GPPCA outperforms the other methods based on both criteria. Note the difference between four methods are smaller in this example. One possible reason is that the range parameters of the kernels are uniformly sampled from $[10, 10^3]$, which makes some factor processes more independent than the ones in Example 2. In this case, the GPPCA and other approaches behave more similarly.

Since the covariance matrices are different in Example 3, we implement the numerical optimization algorithm on the Stiefel manifold (Wen and Yin, 2013) to estimate \mathbf{A} in Theorem 2. Based on this algorithm, the GPPCA is the best method in estimating the factor loading matrix among all the approaches we consider. However, the numerical optimization

algorithm costs more time than the closed-form solution of the factor loading matrix, when the covariance is shared. Moreover, this solution of the optimization algorithm in Wen and Yin (2013) may also converge to a local optimum. It is an open problem to develop a more efficient and accurate algorithm for the optimization problem in Theorem 2.

$d = 4$ and $\tau = 4$	k=8		k=40	
	$n = 200$	$n = 400$	$n = 200$	$n = 400$
PCA	1.3×10^{-1}	1.3×10^{-1}	3.8×10^{-2}	3.0×10^{-2}
GPPCA	1.6×10^{-2}	1.2×10^{-2}	7.5×10^{-3}	4.4×10^{-3}
LY1	1.6×10^{-1}	1.4×10^{-1}	4.9×10^{-2}	3.4×10^{-2}
LY5	1.5×10^{-1}	1.3×10^{-1}	4.4×10^{-2}	3.2×10^{-2}
$d = 8$ and $\tau = 4$	k=16		k=80	
	$n = 500$	$n = 1000$	$n = 500$	$n = 1000$
PCA	1.3×10^{-1}	1.3×10^{-1}	3.5×10^{-2}	2.9×10^{-2}
GPPCA	1.3×10^{-2}	1.4×10^{-2}	6.0×10^{-3}	4.0×10^{-3}
LY1	1.4×10^{-1}	1.3×10^{-1}	3.7×10^{-2}	3.4×10^{-2}
LY5	1.4×10^{-1}	1.3×10^{-1}	2.9×10^{-2}	2.8×10^{-2}

Table 2: AvgMSE for Example 3.

4.2 Misspecified model

In this subsection, we discuss two numerical examples where the latent factor model is misspecified. First, we have the Assumption 1 due to the identification reason, and it may seem to be restrictive. In both examples, we assume each entry of the factor loading matrix is sampled from a uniform distribution not constrained in the Stiefel manifold. The second misspecification may come from the misuse of the kernel function in the factor processes. In reality, the smoothness of the true process may be unknown so using any particular type of the kernel may lead to under-smoothing or over-smoothing. Moreover, the factor may be an unknown deterministic function, rather than a sample from a Gaussian process. All these possible misspecifications will be discussed using the following Example 4 and Example 5.

Example 4 (Unconstrained factor loading matrix and misspecified kernel functions). *The data is sampled from model (1) with $\Sigma_1 = \dots = \Sigma_1 = \Sigma$ where x is equally spaced from 1 to n . Each entry of the factor loading matrix is assumed to be uniformly sampled from $[0, 1]$ (without the orthogonal constraints in (4)). The exponential kernel and the Gaussian kernel are assumed in generating the data with different combinations of σ_0^2 and n , while in the GPPCA, we still use the Matérn kernel function in (12) for the estimation. We assume $k = 20$, $d = 4$, $\gamma = 100$ and $\sigma^2 = 1$ in sampling the data. We repeat $N = 100$ times for each scenario. All the kernel parameters and the variance of the noise are treated as unknown and estimated from the data.*

The last principal angles between $\mathcal{M}(\mathbf{A})$ and $\mathcal{M}(\hat{\mathbf{A}})$ of the four approaches for Example 4 are graphed in Figure 6. Even though the factor loading matrix is not constrained on

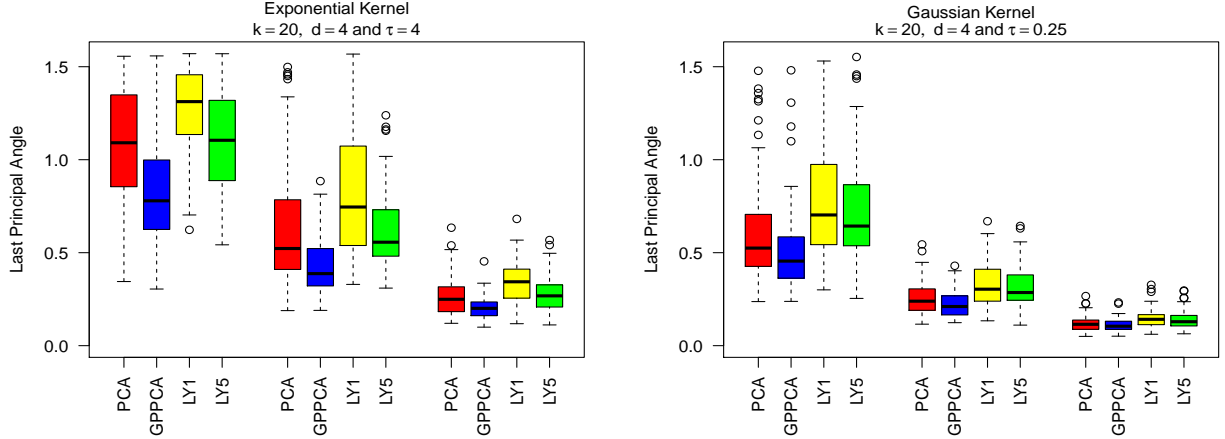


Figure 6: The last principal angle between the estimated subspace of four approaches and the true subspace for Example 4. The number of observations are assumed to be $n = 100$, $n = 200$ and $n = 400$ for left 4 boxplots, middle 4 boxplots and right 4 boxplots in both panels, respectively. The kernel in simulating the data is assumed to be the exponential kernel in the left panel, whereas the kernel is assumed to be the Gaussian kernel in the right panel.

the Stiefel manifold and the kernels are misused in GPPCA, the estimation of the GPPCA is still better than other approaches in all scenarios. The PCA is an extreme case of the GPPCA where the range parameter of the kernel is estimated to be zero, meaning that the covariance of the factor process is an identity matrix. Even one missues a kernel function in the GPPCA, it still performs better than assuming all factors are independent.

Another interesting finding is that all methods seem to perform better when the Gaussian kernel is used in simulating the data, even if the SNR of the simulation using a Gaussian kernel is smaller. This is because the variation of the factors is much larger when the Gaussian kernel is used, which makes the effect of the noise relatively small. In both cases, the GPPCA seems to be efficient in estimating the subspace of the factor loading matrix.

Furthermore, since only the linear subspace of the factor loading matrix is identifiable, rather than the factor loading matrix, the estimation of the factor loadings without the orthogonal constraints is also accurate by the GPPCA. Note the interpretation of the estimated variance parameter in the kernel by the GPPCA changes, because each column of \mathbf{A} is not orthonormal in generating the data.

The AvgMSE of the four approaches for Example 4 is shown in Table 3. The estimation of the GPPCA is more accurate than the other approaches. Because of the larger variation in the factor processes with the Gaussian kernel, the corresponding variation in the mean of the output is also larger than the one when the exponential kernel is used. Consequently, all approaches have larger estimated errors for the case with the Gaussian kernel.

We discuss the last example where the factor is assumed to be the output from a deterministic function as follows.

Example 5 (Unconstrained factor loading matrix and deterministic factors). *The data is*

	exponential kernel and $\tau = 4$			Gaussian kernel and $\tau = 1/4$		
	$n = 100$	$n = 200$	$n = 400$	$n = 100$	$n = 200$	$n = 400$
PCA	7.4×10^{-2}	6.1×10^{-2}	5.4×10^{-2}	1.1×10^0	8.9×10^{-1}	8.4×10^{-1}
GPPCA	3.1×10^{-2}	2.6×10^{-2}	2.4×10^{-2}	7.2×10^{-1}	6.8×10^{-1}	6.4×10^{-1}
LY1	1.5×10^{-1}	8.2×10^{-1}	5.7×10^{-2}	1.3×10^0	1.0×10^0	8.6×10^{-1}
LY5	1.3×10^{-1}	7.3×10^{-1}	5.6×10^{-2}	1.3×10^0	1.0×10^0	8.6×10^{-1}

Table 3: AvgMSE for Example 4.

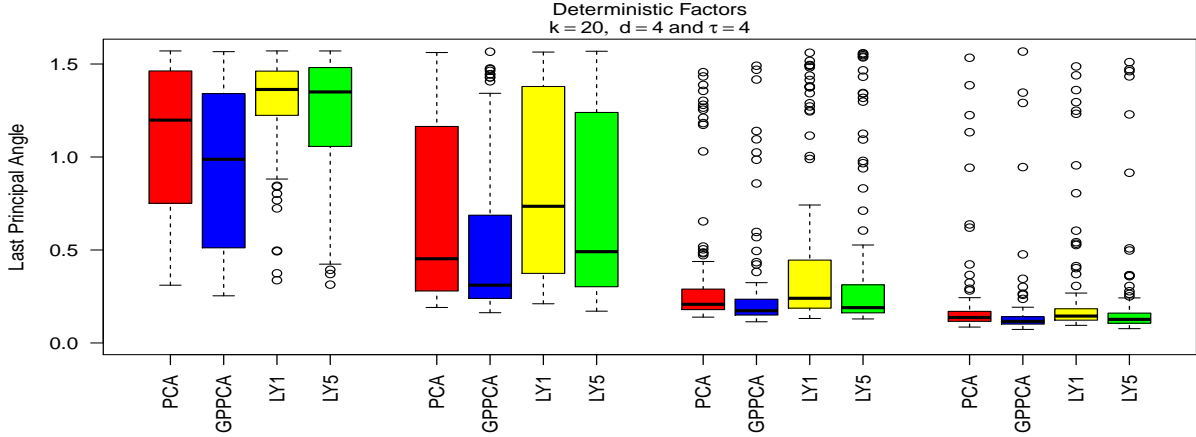


Figure 7: The last principal angle between the estimated subspace of the loading matrix and the true subspace for Example 5. From the left to the right, the number of observations are assumed to be $n = 100$, $n = 200$, $n = 400$ and $n = 800$ for each 4 boxplots, respectively.

sampld from model (1) with each latent factor follows a deterministic function

$$Z_l(x_i) = \cos(0.05\pi\theta_l x_i)$$

where $\theta_l \stackrel{i.i.d.}{\sim} \text{unif}(0, 1)$ for $l = 1, \dots, d$, with x_i equally spaced from 1 to n , $\sigma_0^2 = 0.25$, $k = 20$ and $d = 4$. Four scenarios are tested with the sample size $n = 100$, $n = 200$, $n = 400$ and $n = 800$.

For the GPPCA, we assume the covariance is shared for each factor and the Matérn kernel in (12) is used for Example 5. The last principal angle between $\mathcal{M}(\mathbf{A})$ and $\mathcal{M}(\hat{\mathbf{A}})$ of the four approaches is given in Figure 7. When the number of observations increase, it seems all methods estimate $\mathcal{M}(\mathbf{A})$ more accurately, even though the factors are no longer sampled from Gaussian processes. Note the reproducing kernel Hilbert space attached to the Gaussian process with the Matérn kernel contains the functions in the Sobolev space that are squared integrable up to the order 2 (Gu et al. (2018c)), while the deterministic function to generate the factors in Example 5 is infinitely integrable. The estimation by the GPPCA is still the best approach in estimating $\mathcal{M}(\mathbf{A})$ among the four approaches in this scenario.

The AvgMSE of the different approaches in estimating the mean of the output of the

	$n = 100$	$n = 200$	$n = 400$	$n = 800$
PCA	7.0×10^{-2}	6.0×10^{-2}	5.4×10^{-2}	5.2×10^{-2}
GPPCA	1.4×10^{-2}	8.9×10^{-3}	6.4×10^{-3}	5.2×10^{-3}
LY1	9.8×10^{-1}	7.6×10^{-1}	6.3×10^{-2}	5.7×10^{-2}
LY5	9.3×10^{-2}	7.2×10^{-2}	6.3×10^{-2}	5.6×10^{-2}
Ind GP	2.0×10^{-2}	1.9×10^{-2}	1.7×10^{-2}	1.7×10^{-2}
PP GP	2.0×10^{-2}	1.9×10^{-2}	1.8×10^{-2}	1.8×10^{-2}

Table 4: AvgMSE for Example 5.

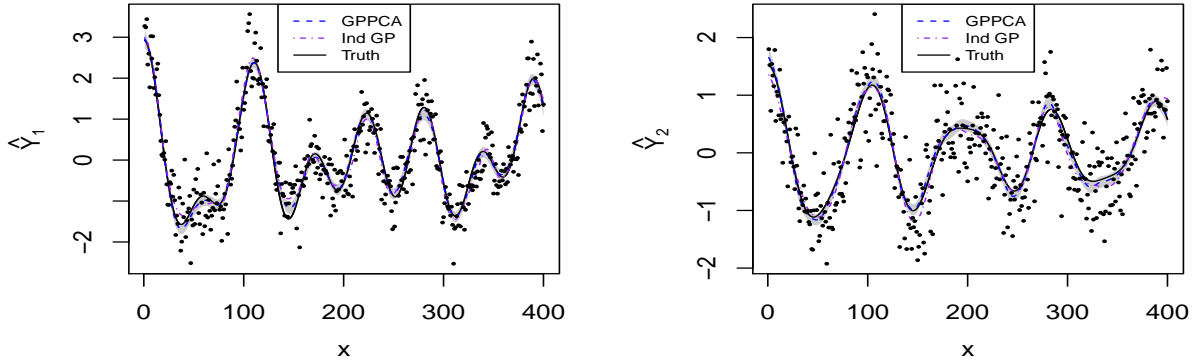


Figure 8: Estimation of the mean of the first two rows of output in one experiment in Example 5 with $n = 400$ and $\tau = 4$. The observations are plotted as black curves and the truth is graphed as the black curves. The estimation by PCA, GPPCA and independent GaSP regression are graphed as the red dotted curves, blue dashed curves and purple dashed curves respectively. The shaded area is the 95% posterior credible interval by GPPCA.

Example 5 is given in Table 4. We also include two more approaches, namely the independent Gaussian processes (Ind GP) and the parallel partial Gaussian processes (PP GP). The Ind GP approach treats each output variable independently and the mean of the output is estimated by the predictive mean in the Gaussian process regression (Rasmussen (2006)). The PP GP approach also models each output variable independently by a Gaussian process, whereas the covariance function is shared for k independent Gaussian processes and estimated based on all data (Gu and Berger (2016)).

As shown in Table 4, the estimation by the GPPCA is the most accurate one among six approaches. The estimation by the Ind GP and PP GP perform similarly and they seem to perform better than the estimation by the PCA, LY1 and LY5. One interesting thing in Table 4 is that the AvgMSE by the GPPCA seems to decrease faster than the ones by the Ind GP and PP GP, when the sample size increases. This numerical result may shed some lights on the convergence rate of the GPPCA in the nonparametric regression problem for multiple functions.

The estimation of the mean of the first two output variables by the GPPCA and Ind GP

in one experiment of Example 5 is graphed in Figure 8. Both seem to perform reasonably well. The 95% posterior credible interval by the GPPCA also seems to be relatively accurate in this example.

5 Concluding remarks

We have introduced the GPPCA, as an extension of the PPCA for the latent factor model with the correlated factors. By allowing data to infer the covariance structure of the factors, the estimation of the factor loading matrix and the mean of the output variables both becomes more accurate by the GPPCA, compared to the PCA and other approaches. This work also highlights the scalable computation achieved by a closed-form expression of the precision matrix in the marginal likelihood. We use the Gaussian processes to model the factor processes for the demonstration purpose, and the results are applicable to many other ways of modeling the covariance structure of the factors.

There are several future directions related to this work. First of all, the factor loading matrix, as well as other parameters in the kernel functions and the variance of the noise, is estimated by the maximum marginal likelihood estimator, where the uncertainty in the parameter estimation is not expressed in the predictive distribution of the output variables. A full Bayesian approach requires a reasonable prior of the factor loading matrix on the Stiefel manifold and the other parameters in the model, which can quantify the uncertainty of the predictive distribution. Secondly, we assume the number of the latent factors is known in this work, and a consistent way to identify the number of latent factors is often needed in practice. Furthermore, the convergence rate of the predictive distribution and the estimation of the subspace of the factor loading matrix of the GPPCA both need to be explored. The numerical results shown in this work seem to be encouraging towards this direction. Besides, a computationally feasible way that combines useful covariates in the data might also be helpful in some applications. Lastly, when the covariances of the factor processes are not the same, the numerical optimization algorithm that preserves the orthogonal constraints (Wen and Yin (2013)) is implemented for the marginal maximum likelihood estimator of the factor loading matrix. The convergence of this algorithm is an interesting direction to explore. A faster and more accurate algorithm for the optimization problem in Theorem 2 will also be crucial for some computationally intensive applications.

Appendix A: Auxiliary facts

1. Let \mathbf{A} and \mathbf{B} be matrices,

$$(\mathbf{A} \otimes \mathbf{B})^T = (\mathbf{A}^T \otimes \mathbf{B}^T);$$

further assuming \mathbf{A} and \mathbf{B} are invertible,

$$(\mathbf{A} \otimes \mathbf{B})^{-1} = \mathbf{A}^{-1} \otimes \mathbf{B}^{-1}.$$

2. Let \mathbf{A} , \mathbf{B} , \mathbf{C} and \mathbf{D} be the matrices such that the products \mathbf{AC} and \mathbf{BD} are matrices,

$$(\mathbf{A} \otimes \mathbf{B})(\mathbf{C} \otimes \mathbf{D}) = (\mathbf{AC}) \otimes (\mathbf{BD}).$$

3. For matrices \mathbf{A} , \mathbf{B} and \mathbf{C} ,

$$(\mathbf{C}^T \otimes \mathbf{A})\text{vec}(\mathbf{B}) = \text{vec}(\mathbf{ABC});$$

further assuming $\mathbf{A}^T \mathbf{B}$ is a matrix,

$$\text{tr}(\mathbf{A}^T \mathbf{B}) = \text{vec}(\mathbf{A})^T \text{vec}(\mathbf{B}).$$

Appendix B: Proofs

We first give some notations for the vectorization used in the proofs. Let $\mathbf{A}_v = [\mathbf{I}_n \times \mathbf{a}_1, \dots, \mathbf{I}_n \times \mathbf{a}_d]$ and $\mathbf{Z}_v = \text{vec}(\mathbf{Z})$. Let $\mathbf{\Sigma}_v$ be a $nd \times nd$ block diagonal matrix where the l th diagonal block is $\mathbf{\Sigma}_l$, for $l = 1, \dots, d$.

Proof of Equation (3). Vectorize the observations in model (1), one has

$$\mathbf{Y}_v = \mathbf{A}_v \mathbf{Z}_v + \boldsymbol{\epsilon}_v$$

where $\mathbf{Z}_v \sim N(\mathbf{0}, \mathbf{\Sigma}_v)$ and $\boldsymbol{\epsilon}_v \sim N(\mathbf{0}, \sigma^2 \mathbf{I}_{nk})$. Using the fact 1 and fact 2, $\mathbf{A}_v \mathbf{Z}_v \sim \text{MN}(\mathbf{0}, \mathbf{\Sigma}_{A_v Z_v})$, where

$$\begin{aligned} \mathbf{\Sigma}_{A_v Z_v} &= \mathbf{A}_v \mathbf{\Sigma}_v \mathbf{A}_v^T \\ &= [\mathbf{\Sigma}_1 \otimes \mathbf{a}_1, \dots, \mathbf{\Sigma}_d \otimes \mathbf{a}_d] \mathbf{A}_v^T \\ &= \sum_{l=1}^d \mathbf{\Sigma}_l \otimes (\mathbf{a}_l \mathbf{a}_l^T), \end{aligned} \tag{19}$$

for $l = 1, \dots, d$. Marginalizing out \mathbf{Z}_v , one has Equation (3). □

Proof of Lemma 1. By (3) and (19), one has

$$\mathbf{Y}_v \mid \mathbf{A}, \sigma_0^2, \mathbf{\Sigma}_1, \dots, \mathbf{\Sigma}_d \sim \text{MN}(\mathbf{0}, \mathbf{A}_v \mathbf{\Sigma}_v \mathbf{A}_v^T + \sigma_0^2 \mathbf{I}_{nk}).$$

The precision matrix is

$$\begin{aligned}
& (\mathbf{A}_v \boldsymbol{\Sigma}_v \mathbf{A}_v^T + \sigma_0^2 \mathbf{I}_{nk})^{-1} \\
&= \sigma_0^{-2} \mathbf{I}_{nk} - \mathbf{A}_v \frac{(\sigma_0^2 \boldsymbol{\Sigma}_v^{-1} + \mathbf{A}_v \mathbf{A}_v^T)^{-1}}{\sigma_0^2} \mathbf{A}_v^T \\
&= \sigma_0^{-2} \mathbf{I}_{nk} - \mathbf{A}_v \frac{(\sigma_0^2 \boldsymbol{\Sigma}_v^{-1} + \mathbf{I}_{nk})^{-1}}{\sigma_0^2} \mathbf{A}_v^T \\
&= \sigma_0^{-2} \left\{ \mathbf{I}_{nk} - [(\sigma_0^2 \boldsymbol{\Sigma}_1^{-1} + \mathbf{I}_n)^{-1} \otimes \mathbf{a}_1, \dots, (\sigma_0^2 \boldsymbol{\Sigma}_d^{-1} + \mathbf{I}_n)^{-1} \otimes \mathbf{a}_d] \mathbf{A}_v^T \right\} \\
&= \sigma_0^{-2} \left(\mathbf{I}_{nk} - \sum_{l=1}^d (\sigma_0^2 \boldsymbol{\Sigma}_l^{-1} + \mathbf{I}_n)^{-1} \otimes \mathbf{a}_l \mathbf{a}_l^T \right)
\end{aligned}$$

where the first equality follows from the Woodbury identity; the second equality is by Assumption 1; the third equality is by fact 2; and the fourth equality is by fact 1 and fact 2, from which the results follow immediately. \square

Proof of Theorem 1. When $\boldsymbol{\Sigma}_1 = \dots = \boldsymbol{\Sigma}_d = \boldsymbol{\Sigma}$, by the fact 3, the likelihood of \mathbf{A} is

$$\begin{aligned}
L(\mathbf{A} \mid \mathbf{Y}, \sigma_0^2, \boldsymbol{\Sigma}) &\propto \exp \left(- \frac{\mathbf{Y}_v^T \left(\mathbf{I}_{nk} - (\sigma_0^2 \boldsymbol{\Sigma}^{-1} + \mathbf{I}_n)^{-1} \otimes \sum_{l=1}^d \mathbf{a}_l \mathbf{a}_l^T \right) \mathbf{Y}_v}{2\sigma_0^2} \right) \\
&\propto \exp \left(- \frac{\mathbf{Y}_v^T \mathbf{Y}_v - \mathbf{Y}_v^T \text{vec}(\mathbf{A} \mathbf{A}^T \mathbf{Y} (\sigma_0^2 \boldsymbol{\Sigma}^{-1} + \mathbf{I}_n)^{-1})}{2\sigma_0^2} \right) \\
&\propto \text{etr} \left(- \frac{\mathbf{Y}^T \mathbf{Y} - \mathbf{Y}^T \mathbf{A} \mathbf{A}^T \mathbf{Y} (\sigma_0^2 \boldsymbol{\Sigma}^{-1} + \mathbf{I}_n)^{-1}}{2\sigma_0^2} \right) \\
&\propto \text{etr} \left(- \frac{\mathbf{Y}^T \mathbf{Y} - \mathbf{A}^T \mathbf{Y} (\sigma_0^2 \boldsymbol{\Sigma}^{-1} + \mathbf{I}_n)^{-1} \mathbf{Y}^T \mathbf{A}}{2\sigma_0^2} \right),
\end{aligned}$$

where $\text{etr}(\cdot) := \exp(\text{tr}(\cdot))$.

Maximizing the likelihood as a function of \mathbf{A} is equivalent to the following optimization problem

$$\hat{\mathbf{A}} = \underset{\mathbf{A}}{\text{argmax}} \text{tr}(\mathbf{A}^T \mathbf{G} \mathbf{A}) \quad \text{s.t.} \quad \mathbf{A}^T \mathbf{A} = \mathbf{I}_d, \quad (20)$$

where $\mathbf{G} = \mathbf{Y} (\mathbf{I}_n + \sigma_0^2 \boldsymbol{\Sigma}^{-1})^{-1} \mathbf{Y}^T$. This optimization in (20) is a trace optimization problem (Kokopoulou et al. (2011)). By the Courant-Fischer-Weyl min-max principal (Saad (1992)), $\text{tr}(\mathbf{A}^T \mathbf{G} \mathbf{A})$ is maximized when $\hat{\mathbf{A}} = \mathbf{U} \mathbf{R}$, with \mathbf{U} being the orthonormal basis of the eigenspace associated with the d largest eigenvalue of \mathbf{G} and \mathbf{R} is any arbitrary rotation matrix. In this case

$$\text{tr}(\hat{\mathbf{A}}^T \mathbf{G} \hat{\mathbf{A}}) = \text{tr}(\mathbf{U} \boldsymbol{\Lambda} \mathbf{U}^T) = \sum_{l=1}^d \lambda_l.$$

where $\boldsymbol{\Lambda}$ is a diagonal matrix of the d largest eigenvalue λ_l of \mathbf{G} , for $l = 1, \dots, d$. \square

Proof of Theorem 2. Under Assumption 1, by fact 3, the likelihood for \mathbf{A} is

$$\begin{aligned} L(\mathbf{A} \mid \mathbf{Y}, \sigma_0^2, \Sigma_1, \dots, \Sigma_d) &\propto \exp \left(-\frac{\mathbf{Y}_v^T \left(\mathbf{I}_{nk} - \sum_{l=1}^d (\sigma_0^2 \Sigma_l^{-1} + \mathbf{I}_n)^{-1} \otimes \mathbf{a}_l \mathbf{a}_l^T \right) \mathbf{Y}_v}{2\sigma_0^{-2}} \right) \\ &\propto \text{etr} \left(-\frac{\mathbf{Y}^T \mathbf{Y} - \mathbf{Y} \sum_{l=1}^d \mathbf{a}_l \mathbf{a}_l^T \mathbf{Y}^T (\sigma_0^2 \Sigma_l^{-1} + \mathbf{I}_n)^{-1}}{2\sigma_0^2} \right) \\ &\propto \text{etr} \left(-\frac{\mathbf{Y}^T \mathbf{Y} - \sum_{l=1}^d \mathbf{a}_l^T \mathbf{Y}^T (\sigma_0^2 \Sigma_l^{-1} + \mathbf{I}_n)^{-1} \mathbf{Y} \mathbf{a}_l}{2\sigma_0^2} \right), \end{aligned}$$

from which the result follows. \square

Proof of Lemma 2. From the proof of Theorem 2, one has

$$L(\sigma_0^2 \mid \mathbf{Y}, \Sigma_1, \dots, \Sigma_d, \mathbf{A}) \propto (\sigma_0^2)^{-nk/2} \text{etr} \left(-\frac{\mathbf{Y}^T \mathbf{Y} - \sum_{l=1}^d \mathbf{a}_l^T \mathbf{Y}^T (\sigma_0^2 \Sigma_l^{-1} + \mathbf{I}_n)^{-1} \mathbf{Y} \mathbf{a}_l}{2\sigma_0^2} \right). \quad (21)$$

Equation (13) follows immediately by maximizing (21).

We now turn to show the profile likelihood in (14). Under Assumption 1

$$\begin{aligned} &p(\mathbf{Y} \mid \boldsymbol{\tau}, \boldsymbol{\gamma}, \mathbf{A}, \sigma_0^2) \\ &= \int p(\mathbf{Y} \mid \mathbf{A}, \sigma_0^2, \mathbf{Z}) p(\mathbf{Z} \mid \boldsymbol{\tau}, \boldsymbol{\gamma}) d\mathbf{Z} \\ &= \int (2\pi\sigma_0^2)^{-\frac{nk}{2}} \text{etr} \left(-\frac{(\mathbf{Y} - \mathbf{AZ})^T (\mathbf{Y} - \mathbf{AZ})}{\sigma_0^2} \right) (2\pi)^{-\frac{nd}{2}} \prod_{l=1}^d |\Sigma_l|^{-\frac{1}{2}} \exp \left(-\frac{1}{2} \sum_{l=1}^d \mathbf{z}_l^T \Sigma_l^{-1} \mathbf{z}_l \right) d\mathbf{Z} \\ &= (2\pi\sigma_0^2)^{-\frac{nk}{2}} \prod_{l=1}^d |\Sigma_l/\sigma_0^2 + \mathbf{I}_k|^{-1/2} \exp \left(-\frac{S^2}{2\sigma_0^2} \right) \end{aligned} \quad (22)$$

where $S^2 = \text{tr}(\mathbf{Y}^T \mathbf{Y}) - \sum_{l=1}^d \mathbf{a}_l^T \mathbf{Y} (\tilde{\Sigma}_l^{-1} + \mathbf{I}_n)^{-1} \mathbf{Y}^T \mathbf{a}_l$. Equation (14) follows by plugging $\hat{\mathbf{A}}$, $\hat{\boldsymbol{\mu}}$ and $\hat{\sigma}_0^2$ into (22). \square

Proof of Theorem 3. Denote the parameters $\hat{\boldsymbol{\theta}} = (\hat{\boldsymbol{\gamma}}, \hat{\mathbf{A}}, \hat{\boldsymbol{\sigma}}^2, \hat{\sigma}_0^2)$. Denote $\hat{\Sigma}$ as the estimated Σ_v by plugging the estimated parameters. We first compute the posterior distribution of $(\mathbf{Z}_v \mid \mathbf{Y}_v, \hat{\boldsymbol{\theta}})$. From Equation (3),

$$\begin{aligned} p(\mathbf{Z}_v \mid \mathbf{Y}_v, \hat{\boldsymbol{\theta}}) &\propto \exp \left(\frac{(\mathbf{Y}_v - \hat{\mathbf{A}}_v \mathbf{Z}_v)^T (\mathbf{Y}_v - \hat{\mathbf{A}}_v \mathbf{Z}_v)}{2\hat{\sigma}_0^2} \right) \exp \left(-\frac{1}{2} \mathbf{Z}_v^T \hat{\Sigma}_v^{-1} \mathbf{Z}_v \right) \\ &\propto \exp \left\{ -(\mathbf{Z}_v - \hat{\mathbf{Z}}_v)^T \left(\frac{\hat{\mathbf{A}}_v^T \hat{\mathbf{A}}_v}{\hat{\sigma}_0^2} + \hat{\Sigma}_v^{-1} \right) (\mathbf{Z}_v - \hat{\mathbf{Z}}_v) \right\}, \end{aligned}$$

where $\hat{\mathbf{Z}}_v = (\hat{\mathbf{A}}_v^T \hat{\mathbf{A}}_v + \hat{\sigma}_0^2 \hat{\Sigma}_v^{-1})^{-1} \hat{\mathbf{A}}_v^T \mathbf{Y}_v$ from which we have

$$\mathbf{Z}_v \mid \mathbf{Y}_v, \hat{\boldsymbol{\theta}} \sim \text{MN} \left(\hat{\mathbf{Z}}_v, \left(\frac{\hat{\mathbf{A}}_v^T \hat{\mathbf{A}}_v}{\hat{\sigma}_0^2} + \hat{\Sigma}_v^{-1} \right)^{-1} \right). \quad (23)$$

Note $\hat{\mathbf{A}}_v^T \hat{\mathbf{A}}_v = \mathbf{I}_{nd}$. Using fact 2 and fact 3, one has

$$\hat{\mathbf{Z}}_v = \begin{pmatrix} \left(\hat{\sigma}_0^2 \hat{\Sigma}_1^{-1} + \mathbf{I}_n \right)^{-1} \otimes \hat{\mathbf{a}}_1^T \\ \vdots \\ \left(\hat{\sigma}_0^2 \hat{\Sigma}_d^{-1} + \mathbf{I}_n \right)^{-1} \otimes \hat{\mathbf{a}}_d^T \end{pmatrix} \text{vec}(\mathbf{Y}) = \text{vec} \begin{pmatrix} \hat{\mathbf{a}}_1^T \mathbf{Y} \left(\hat{\sigma}_0^2 \hat{\Sigma}_1^{-1} + \mathbf{I}_n \right)^{-1} \\ \vdots \\ \hat{\mathbf{a}}_d^T \mathbf{Y} \left(\hat{\sigma}_0^2 \hat{\Sigma}_d^{-1} + \mathbf{I}_n \right)^{-1} \end{pmatrix} := \text{vec}(\hat{\mathbf{Z}}). \quad (24)$$

Now we are ready to derive the predictive mean and predictive variance. First

$$\begin{aligned} \mathbb{E}[\mathbf{Y}(\mathbf{x}^*) \mid \mathbf{Y}, \hat{\boldsymbol{\theta}}] &= \mathbb{E}[\mathbb{E}[\mathbf{Y}(\mathbf{x}^*) \mid \mathbf{Y}, \mathbf{Z}(\mathbf{x}^*), \hat{\boldsymbol{\theta}}]] = \mathbb{E}[\hat{\mathbf{A}}\mathbf{Z}(\mathbf{x}^*) \mid \mathbf{Y}, \hat{\boldsymbol{\theta}}] \\ &= \hat{\mathbf{A}} \mathbb{E}[\mathbb{E}[\mathbf{Z}(\mathbf{x}^*) \mid \mathbf{Y}, \mathbf{Z}, \hat{\boldsymbol{\theta}}]] = \hat{\mathbf{A}} \hat{\mathbf{Z}}(\mathbf{x}^*) \end{aligned}$$

with the l th term of $\hat{\mathbf{Z}}(\mathbf{x}^*)$

$$\begin{aligned} \hat{Z}_l(\mathbf{x}^*) &= \hat{\Sigma}_l(\mathbf{x}^*) \Sigma_l^{-1} \mathbb{E}[\mathbf{Z}_l^T \mid \mathbf{Y}, \hat{\boldsymbol{\theta}}] \\ &= \hat{\Sigma}_l(\mathbf{x}^*) \hat{\Sigma}_l^{-1} (\hat{\Sigma}_l^{-1} + \hat{\sigma}_0^2 \mathbf{I}_n)^{-1} \mathbf{Y} \hat{\mathbf{a}}_l \\ &= \hat{\Sigma}_l(\mathbf{x}^*) (\hat{\sigma}_0^2 \mathbf{I}_n + \hat{\Sigma}_l)^{-1} \mathbf{Y} \hat{\mathbf{a}}_l. \end{aligned}$$

where the first equality is from the property of multivariate normal distribution and the second equality is from (24).

Secondly, we have

$$\begin{aligned} &\mathbb{V}[\mathbf{Y}^* \mid \mathbf{Y}, \hat{\boldsymbol{\theta}}] \\ &= \mathbb{E}[\mathbb{V}[\mathbf{Y}^* \mid \mathbf{Y}, \hat{\boldsymbol{\theta}}, \mathbf{Z}(\mathbf{x}^*)]] + \mathbb{V}[\mathbb{E}[\mathbf{Y}^* \mid \mathbf{Y}, \hat{\boldsymbol{\theta}}, \mathbf{Z}(\mathbf{x}^*)]] \\ &= \hat{\sigma}_0^2 \mathbf{I}_k + \mathbb{V}[\hat{\mathbf{A}}\mathbf{Z}(\mathbf{x}^*) \mid \mathbf{Y}, \hat{\boldsymbol{\theta}}] \\ &= \hat{\sigma}_0^2 \mathbf{I}_k + \hat{\mathbf{A}} [\mathbb{E}[\mathbb{V}[\mathbf{Z}(\mathbf{x}^*) \mid \mathbf{Y}, \hat{\boldsymbol{\theta}}, \mathbf{Z}]] + \mathbb{V}[\mathbb{E}[\mathbf{Z}(\mathbf{x}^*) \mid \mathbf{Y}, \hat{\boldsymbol{\theta}}, \mathbf{Z}]]] \hat{\mathbf{A}}^T = \hat{\sigma}_0^2 \mathbf{I}_k + \hat{\sigma}_0^2 \hat{\mathbf{A}} \hat{\mathbf{D}}(\mathbf{x}^*) \hat{\mathbf{A}}^T \end{aligned}$$

with

$$\begin{aligned}
\hat{\mathbf{D}}(\mathbf{x}^*) &= \frac{1}{\hat{\sigma}_0^2} (\mathbb{E}[\mathbb{V}[\mathbf{Z}(\mathbf{x}^*) \mid \mathbf{Y}, \hat{\boldsymbol{\theta}}, \mathbf{Z}]] + \mathbb{V}[\mathbb{E}[\mathbf{Z}(\mathbf{x}^*) \mid \mathbf{Y}, \hat{\boldsymbol{\theta}}, \mathbf{Z}]]) \\
&= \frac{1}{\hat{\sigma}_0^2} \begin{pmatrix} \hat{K}_1(\mathbf{x}^*, \mathbf{x}^*) - \hat{\Sigma}_1(\mathbf{x}^*)^T \hat{\Sigma}_1^{-1} \hat{\Sigma}_1(\mathbf{x}^*) \\ \vdots \\ \hat{K}_d(\mathbf{x}^*, \mathbf{x}^*) - \hat{\Sigma}_d(\mathbf{x}^*)^T \hat{\Sigma}_d^{-1} \hat{\Sigma}_d(\mathbf{x}^*) \end{pmatrix} + \frac{1}{\hat{\sigma}_0^2} \begin{pmatrix} \hat{\Sigma}_1(\mathbf{x}^*)^T \hat{\Sigma}_1^{-1} (\hat{\Sigma}_1^{-1} + \frac{\mathbf{I}_n}{\hat{\sigma}_0^2})^{-1} \hat{\Sigma}_1^{-1} \hat{\Sigma}_1(\mathbf{x}^*) \\ \vdots \\ \hat{\Sigma}_d(\mathbf{x}^*)^T \hat{\Sigma}_d^{-1} (\hat{\Sigma}_d^{-1} + \frac{\mathbf{I}_n}{\hat{\sigma}_0^2})^{-1} \hat{\Sigma}_d^{-1} \hat{\Sigma}_d(\mathbf{x}^*) \end{pmatrix} \\
&= \frac{1}{\hat{\sigma}_0^2} \begin{pmatrix} \hat{K}_1(\mathbf{x}^*, \mathbf{x}^*) - \hat{\Sigma}_1(\mathbf{x}^*)^T (\hat{\sigma}_0^2 \mathbf{I}_n + \hat{\Sigma}_1)^{-1} \hat{\Sigma}_1(\mathbf{x}^*) \\ \vdots \\ \hat{K}_d(\mathbf{x}^*, \mathbf{x}^*) - \hat{\Sigma}_d(\mathbf{x}^*)^T (\hat{\sigma}_0^2 \mathbf{I}_n + \hat{\Sigma}_d)^{-1} \hat{\Sigma}_d(\mathbf{x}^*) \end{pmatrix}
\end{aligned}$$

where the first equality is from the property of the multivariate normal distribution and (23); the second equality is from the Woodbury Identity. \square

References

- Álvarez, M. A., Rosasco, L., and Lawrence, N. D. (2011). Kernels for vector-valued functions: a review. *arXiv preprint arXiv:1106.6251*.
- Bai, J. (2003). Inferential theory for factor models of large dimensions. *Econometrica*, 71(1):135–171.
- Bai, J. and Ng, S. (2002). Determining the number of factors in approximate factor models. *Econometrica*, 70(1):191–221.
- Bhattacharya, A. and Dunson, D. B. (2011). Sparse bayesian infinite factor models. *Biometrika*, pages 291–306.
- Björck, . and Golub, G. H. (1973). Numerical methods for computing angles between linear subspaces. *Mathematics of computation*, 27(123):579–594.
- Conti, S. and O’Hagan, A. (2010). Bayesian emulation of complex multi-output and dynamic computer models. *Journal of statistical planning and inference*, 140(3):640–651.
- Fricker, T. E., Oakley, J. E., and Urban, N. M. (2013). Multivariate gaussian process emulators with nonseparable covariance structures. *Technometrics*, 55(1):47–56.
- Gelfand, A. E., Diggle, P., Guttorp, P., and Fuentes, M. (2010). *Handbook of spatial statistics*. CRC Press.
- Gelfand, A. E., Schmidt, A. M., Banerjee, S., and Sirmans, C. (2004). Nonstationary multivariate process modeling through spatially varying coregionalization. *Test*, 13(2):263–312.
- Gu, M. and Berger, J. O. (2016). Parallel partial Gaussian process emulation for computer models with massive output. *Annals of Applied Statistics*, 10(3):1317–1347.

- Gu, M., Palomo, J., and Berger, J. O. (2018a). Robustgasp: Robust Gaussian stochastic process emulation in r. *arXiv preprint arXiv:1801.01874*.
- Gu, M., Wang, X., and Berger, J. O. (2018b). Robust Gaussian stochastic process emulation. *Annals of Statistics, In Press. arXiv preprint arXiv:1708.04738*.
- Gu, M., Xie, F., and Wang, L. (2018c). A theoretical framework of the scaled Gaussian stochastic process in prediction and calibration. *arXiv preprint arXiv:1807.03829*.
- Gu, M. and Xu, Y. (2017). Nonseparable Gaussian stochastic process: A unified view and computational strategy. *arXiv preprint arXiv:1711.11501*.
- Hartikainen, J. and Sarkka, S. (2010). Kalman filtering and smoothing solutions to temporal gaussian process regression models. In *Machine Learning for Signal Processing (MLSP), 2010 IEEE International Workshop on*, pages 379–384. IEEE.
- Higdon, D., Gattiker, J., Williams, B., and Rightley, M. (2008). Computer model calibration using high-dimensional output. *Journal of the American Statistical Association*, 103(482):570–583.
- Hoff, P. (2018). *rstiefel: Random Orthonormal Matrix Generation and Optimization on the Stiefel Manifold*. R package version 0.20.
- Jolliffe, I. (2011). Principal component analysis. In *International encyclopedia of statistical science*, pages 1094–1096. Springer.
- Kokopoulou, E., Chen, J., and Saad, Y. (2011). Trace optimization and eigenproblems in dimension reduction methods. *Numerical Linear Algebra with Applications*, 18(3):565–602.
- Lam, C. and Yao, Q. (2012). Factor modeling for high-dimensional time series: inference for the number of factors. *The Annals of Statistics*, 40(2):694–726.
- Lam, C., Yao, Q., and Bathia, N. (2011). Estimation of latent factors for high-dimensional time series. *Biometrika*, 98(4):901–918.
- Nakajima, J. and West, M. (2013). Bayesian analysis of latent threshold dynamic models. *Journal of Business & Economic Statistics*, 31(2):151–164.
- Nocedal, J. (1980). Updating quasi-newton matrices with limited storage. *Mathematics of computation*, 35(151):773–782.
- Oakley, J. (1999). *Bayesian uncertainty analysis for complex computer codes*. PhD thesis, University of Sheffield.
- Rasmussen, C. E. (2006). *Gaussian processes for machine learning*. MIT Press.
- Reynkens, T. (2018). *Robust Sparse PCA using the ROSPCA Algorithm*. R package version 1.0.4.

- Saad, Y. (1992). *Numerical methods for large eigenvalue problems*. Manchester University Press.
- Sacks, J., Welch, W. J., Mitchell, T. J., Wynn, H. P., et al. (1989). Design and analysis of computer experiments. *Statistical science*, 4(4):409–423.
- Seeger, M., Teh, Y.-W., and Jordan, M. (2005). Semiparametric latent factor models. Technical report.
- Tipping, M. E. and Bishop, C. M. (1999). Probabilistic principal component analysis. *Journal of the Royal Statistical Society: Series B (Statistical Methodology)*, 61(3):611–622.
- Wen, Z. and Yin, W. (2013). A feasible method for optimization with orthogonality constraints. *Mathematical Programming*, 142(1-2):397–434.
- West, M. (2003). Bayesian factor regression models in the “large p, small n” paradigm. In Bernardo, J. M., Bayarri, M. J., Berger, J. O., David, A. P., Heckerman, D., Smith, A. F. M., and West, M., editors, *Bayesian Statistics 7*, pages 723–732. Oxford University Press.
- Zhou, X., Nakajima, J., and West, M. (2014). Bayesian forecasting and portfolio decisions using dynamic dependent sparse factor models. *International Journal of Forecasting*, 30(4):963–980.